

Investigating Use of Low-Cost Sensors to Increase Accuracy and Equity of Real-Time Air Quality Information

Ellen M. Considine*¹, Danielle Braun^{1,2}, Leila Kamareddine¹, Rachel C. Nethery⁺¹, and Priyanka deSouza⁺³

¹ Department of Biostatistics, Harvard T.H. Chan School of Public Health

² Department of Data Science, Dana-Farber Cancer Institute

³ Department of Urban and Regional Planning, University of Colorado Denver

⁺ These authors contributed equally to this work.

* Corresponding author contact: ellen_considine@g.harvard.edu

1. Abstract

Environmental Protection Agency (EPA) air quality (AQ) monitors, the gold standard for measuring air pollutants, are sparsely positioned across the US due to their costliness. Low-cost sensors (LCS) are increasingly being used by the public to fill in the gaps in AQ monitoring; however, LCS are not as accurate as EPA monitors. In this work, we investigate factors impacting the differences between an individual's true (unobserved) exposure to fine particulate matter (PM_{2.5}) and the exposure reported by their nearest AQ instrument, which could be either an EPA monitor or an LCS. Three factors contributing to these differences are (1) distance to the nearest AQ instrument, (2) local variability in AQ, and (3) device measurement error. We examine the contributions of each component to the overall error in reported AQ using simulations based on California data. The simulations explore different combinations of hypothetical LCS placement strategies (at schools, near major roads, and in environmentally and socioeconomically marginalized census tracts) for different numbers of LCS, with varying plausible amounts of LCS device measurement error. For each scenario, we evaluate the accuracy of daily AQ information available from individuals' nearest AQ instrument with respect to absolute errors and misclassifications of the Air Quality Index, stratified by socioeconomic and demographic characteristics. We illustrate how real-time AQ reporting could be improved (or, in some cases, worsened) by using LCS, both for the population overall and for marginalized communities specifically. This work has implications for the integration of LCS into real-time AQ reporting platforms.

2. Significance

Deployment of low-cost sensors (LCS) has been promoted as a way to improve real-time air quality (AQ) information and further environmental justice efforts, among other uses. However, factors such as device measurement error and biased placement of LCS may diminish their value. To our knowledge, this is the first study to investigate (on a large scale) how deploying LCS impacts access to daily AQ information – both overall and specifically for members of

marginalized groups – and how this impact depends on the spatial distribution and accuracy of the LCS. Our identification and analysis of mechanisms driving errors in daily AQ reporting may help inform future investment in, and implementation of, LCS networks for the public good.

3. Introduction

Decades of research have documented the adverse health impacts of both short- and long-term exposure to air pollution. In this study, we focus on fine particulate matter (PM_{2.5}), an air pollutant that has been associated with various adverse health outcomes (1–3). In the US, although air quality (AQ) across the years has been improving overall, disparities between PM_{2.5} concentrations experienced by subpopulations persist (4–6). In addition, certain parts of the US are experiencing, or are likely to experience, higher air pollution (including PM_{2.5}) from climate-change related events and processes such as exacerbated wildfires and dust storms (7). To develop effective AQ management plans and address key concerns of equity, accurate and high resolution AQ monitoring data are needed.

The Federal Reference Method or Federal Equivalence Method (FRM or FEM) monitors deployed by the US Environmental Protection Agency (EPA) are considered the gold standard for AQ data. However, due to the prohibitively high capital (USD \$10,000+) and operating costs (8) of these instruments, they have been deployed in less than a third of all US counties (9). Even in counties that have an EPA monitor, the often substantial within-county variability in AQ can render measurements unrepresentative of the pollution levels experienced by many residents of the county (10). For example, as these monitors tend to be deployed in more populous locations (11, 12), residents in rural areas tend to be farther away from monitors.

In recent years, low-cost AQ sensors (< USD \$2,500 as defined by the EPA Air Sensor Guidebook (13), but often much cheaper) have been gaining attention as a supplement to FRM/FEM monitoring, and many are deployed by citizens in addition to public and private entities (14). Networks of these sensors can help increase the spatial resolution and frequency of AQ measurements (15). However, the measurements from low-cost sensors (henceforth, LCS) have lower accuracy than EPA monitors, and can be further affected by environmental conditions such as relative humidity, temperature, and aerosol composition (14, 16–18). Recent work has shown that algorithmic correction can reduce the error in LCS, but does not eliminate the problem (19–22). These studies have also highlighted the challenge of developing corrections that are transferable across measurements collected in different locations and/or time periods. Despite these drawbacks, research has shown that LCS can be useful in identifying air pollution hotspots, expanding local awareness about AQ and health, and alerting the public of short-term changes in AQ, which may facilitate reduction of exposure to air pollution, e.g. by individuals choosing not to exercise outdoors on a high pollution day (13, 23–25).

To our knowledge, the question of how incorporating measurements from LCS into real-time reporting systems affects the accuracy of people's AQ information remains unanswered. In addition to sensor measurement error, an important factor that must be considered is the spatial distribution (both density and relative placement) of LCS. In this study, we assume that individuals view AQ data from the nearest instrument – EPA monitor or LCS – (e.g. as shown on a phone app) as their current AQ exposure. Despite the potential for LCS to increase and democratize access to AQ information, a 2021 study found that locations of PurpleAir (one of the most widely used LCS brands, costing around \$250 per sensor) in the US tend to be disproportionately located in neighborhoods that have higher incomes and higher percentages of white residents, compared both to the locations of EPA monitors and to the US overall (14). This suggests that, relative to more privileged groups, residents of marginalized neighborhoods (who, as previously noted, tend to experience worse air quality) may have less access to information about their local AQ, a precursor to adaptive actions which could be taken to protect their health.

In summary, while collection and dissemination of LCS data have been increasing, there is a need for evaluating the impact of integrating LCS data into AQ reporting platforms. In this study, we investigate how altering the number of LCS deployed, amount and type of sensor measurement error, and relative placements of LCS affects the accuracy of daily AQ information available to individuals from their nearest AQ instrument. We focus on $PM_{2.5}$ and base our LCS investigation on PurpleAir sensors.

Our analysis consists first of simulating realistic LCS $PM_{2.5}$ measurements under numerous hypothetical LCS deployment and sensor measurement error scenarios in the state of California. Then, we compare the local AQ information available to individuals in each scenario with that produced by (i) EPA monitors only, as well as (ii) the existing PurpleAir sensor network. We dedicate special attention to evaluating how each scenario impacts disparities in AQ information accuracy for marginalized groups, such as those living in communities with high rates of poverty or with high proportions of nonwhite or Hispanic residents.

In the following subsections 3.1-3.6, we provide an overview of our analysis, followed by more details on the methodology in section 6 (Materials & Methods). Section 4 (Results) includes a comparison of the impact of different types and amounts of sensor measurement error for LCS at current PurpleAir locations, as well as a comparison across different LCS placement strategies and numbers of LCS deployed. Section 5 (Discussion) includes conclusions, limitations, and some ideas for future investigation.

3.1 Study Setting

To evaluate the potential impact of LCS measurements on localized AQ information accuracy, our study leverages real data on EPA monitor locations, PurpleAir LCS locations, sociodemographic and geospatial features in California. Our choice to situate the study in

California was primarily motivated by the California population's widespread LCS uptake (California contains over half of the US's PurpleAir sensors), in part prompted by concerns about increasing air pollution from wildfires (26–29).

To ensure that our simulations account for realistic spatial and temporal variability in $PM_{2.5}$, we assume the “true” (error-free and comprehensive) daily ambient $PM_{2.5}$ concentrations are those obtained from an ensemble model predicting $PM_{2.5}$ exposures daily at 1 km x 1 km in 2016, obtained from Di et al. (2016 is the most recent year for which these predictions are available) (30). These estimates agree well with ground-based reference measurements: the 10-fold cross-validated R^2 is 0.86 for the US overall and 0.80 for the Pacific coast states (including California). We also consider the current locations of EPA monitors (n=154 in California) to be fixed, and in our simulations we set the $PM_{2.5}$ measurements from each of these monitors to be equal to the Di et al. $PM_{2.5}$ estimates at these locations (i.e., we assume that there is no error in the measurements from these monitors).

3.2 Overview: Simulation Procedure

Here is a broad view of our simulation procedure. More details are provided in the following subsections, and in the Materials & Methods section (section 6). For each combination of LCS placement strategy, number of LCS deployed, and type and amount of sensor measurement error, we repeat this procedure 50 times and calculate the average values of the performance metrics (described in subsections 3.6 and 6.3).

1. Using the given placement strategy, select hypothetical locations of LCS
2. For each 1 km x 1 km grid in California, identify the grid centroid's nearest AQ instrument (from among the real EPA monitor locations and hypothetical LCS locations)
3. For each day in 2016, simulate LCS $PM_{2.5}$ measurements by adding simulated device measurement error to the “true” $PM_{2.5}$ estimates from Di et al. at each hypothetical LCS's location
4. Evaluate the accuracy and equity of AQ information observed (based on the measurements from the nearest AQ instrument) across all 475,772 grids in California and 366 days in 2016

3.3 Overview: Selecting LCS Locations

We simulate and evaluate several hypothetical LCS deployment scenarios in California, with LCS placement locations targeting different populations in each scenario. To guide hypothetical LCS deployment strategies focused on environmentally and socially marginalized communities, we leverage the CalEnviroScreen (CES) index, developed by the California Office of Environmental Health Hazard Assessment, which describes both environmental and socioeconomic-demographic marginalization at the Census tract level (31) and its environmental

component (containing information on pollution in the air and water as well as proximity to waste sites, and henceforth referred to as the Pollution Score).

Specifically, we consider the following five hypothetical LCS placement strategies, illustrated in Figure 1: a) at randomly selected real outdoor PurpleAir locations, b) at randomly selected public schools, c) at randomly selected locations favoring proximity to major roads, d) at randomly selected locations favoring high CES Score, and e) at randomly selected locations favoring high Pollution Score. For the last three placement strategies, “favoring” refers to weighted random sampling (respectively using nearby road lengths, CES Score, and Pollution Score as weights) to determine placement locations. We compare each of these placement strategies across different numbers of sensors deployed (between 0 and 1,000). To provide context, average numbers of LCS assigned to the Los Angeles, Sacramento, Imperial counties (a large city, a medium-small city, and a well-known environmental justice focus area) under each placement strategy are provided in the Supplemental Information (SI) Table A.1.

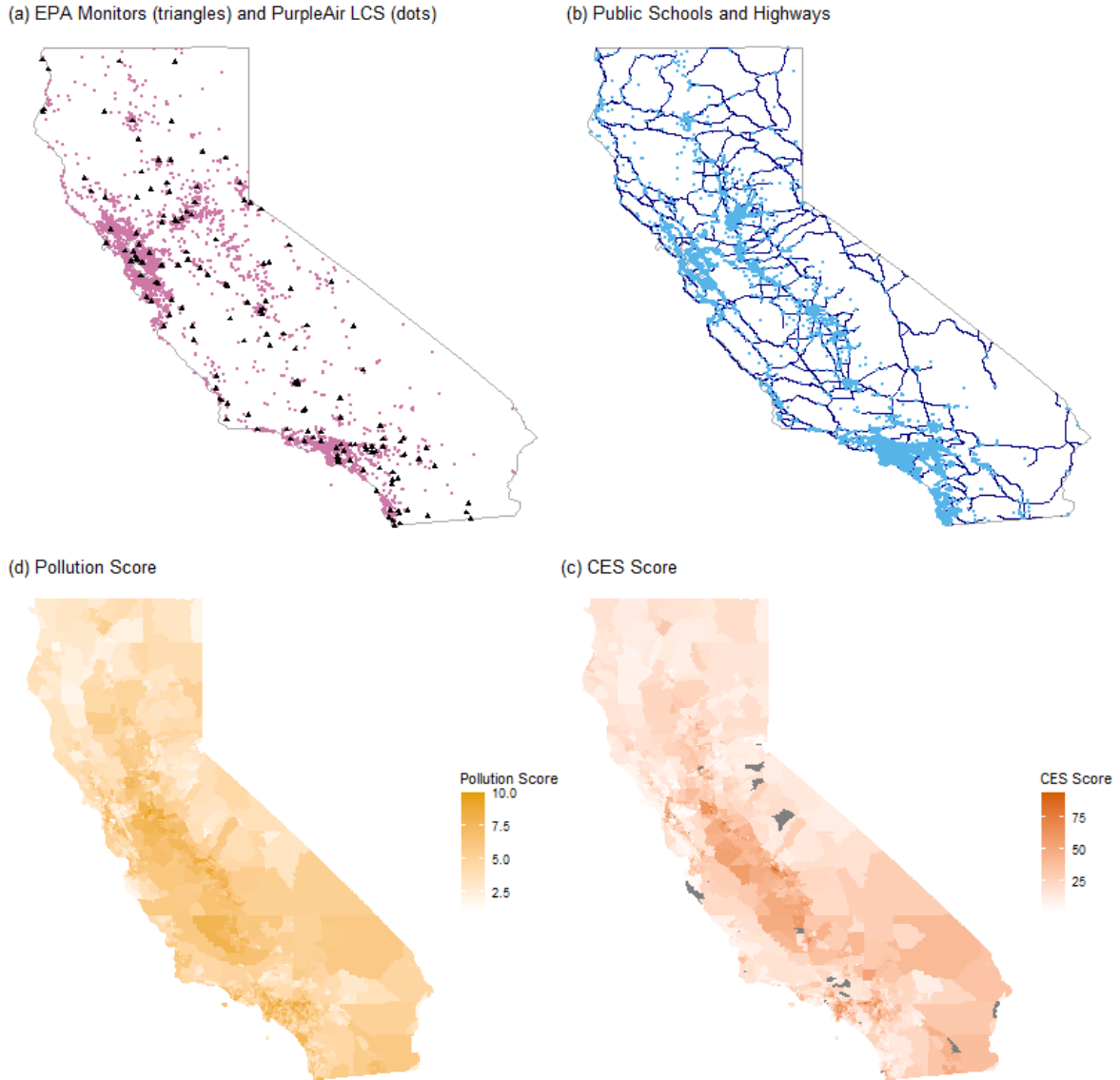


Figure 1: Locations of EPA monitors and PurpleAir LCS (panel a), public schools and major roads in California (panel b), as well as maps of CES (panel c) and Pollution Score (panel d).

3.4 Overview: Simulating Sensor Measurement Error

In each hypothetical (simulated) LCS deployment scenario, daily $\text{PM}_{2.5}$ “measurements” from LCS are generated by adding sensor measurement error to the Di et al. $\text{PM}_{2.5}$ estimates, in several different ways. First, we select measurement error distributions informed by a tiered target for AQ instrument accuracy proposed at an EPA workshop (32). The proposal is that AQ measurements (i) for regulatory purposes require accuracy of $\pm 10\%$ of the true average $\text{PM}_{2.5}$ in that area, (ii) for mapping spatial gradients and monitoring microenvironments require accuracy of $\pm 25\%$, and (iii) for hotspot detection require accuracy of $\pm 50\%$. In our simulations, sensor measurement errors are generated both (a) differentially with respect to true $\text{PM}_{2.5}$ and (b) non-

differentially (with error magnitude not varying across $PM_{2.5}$ levels). The former was motivated by empirical LCS observations.

Second, we simulate LCS measurement errors in a manner that enables assessment of a nationwide correction algorithm for PurpleAir sensors developed by EPA researchers (33). Specifically, we sample errors from the empirical distribution of residuals obtained by comparing measurements from EPA monitors in California to the corrected measurements from collocated PurpleAir sensors.

These procedures are detailed in section 6.2.

3.5 Overview: Observing AQ Information From the Nearest AQ Instrument

We assume that all individuals in each 1 km x 1 km grid in California observe daily AQ measurements from the instrument (either EPA monitor or LCS based on simulated placement strategy) nearest to their grid centroid, as shown in Figure 2. In the True Air Pollution Exposure column (left), the background color in each grid cell represents the “true” air pollution that individuals experience (obtained from the Di et al. estimates). Note that these true exposures are most often not observed. The colors inside the triangles and circles represent the measurements from EPA monitors and LCS, respectively. LCS measurement error is represented in the bottom row, where the color inside the circle differs from the background color of the grid it’s in. In the Shown Air Pollution Exposure column (right), the background color in each grid is the air pollution measurement that individuals observe from their nearest AQ instrument. We now describe the differences between the AQ that individuals experience and are shown, which are indicated by the red and blue X’s in Figure 2. The red X’s indicate cells where AQ is over-classified, i.e., the AQ shown to residents is worse than the AQ truly experienced. The blue X’s indicate cells where AQ is under-classified, i.e., the AQ shown to residents is better than the AQ truly experienced.

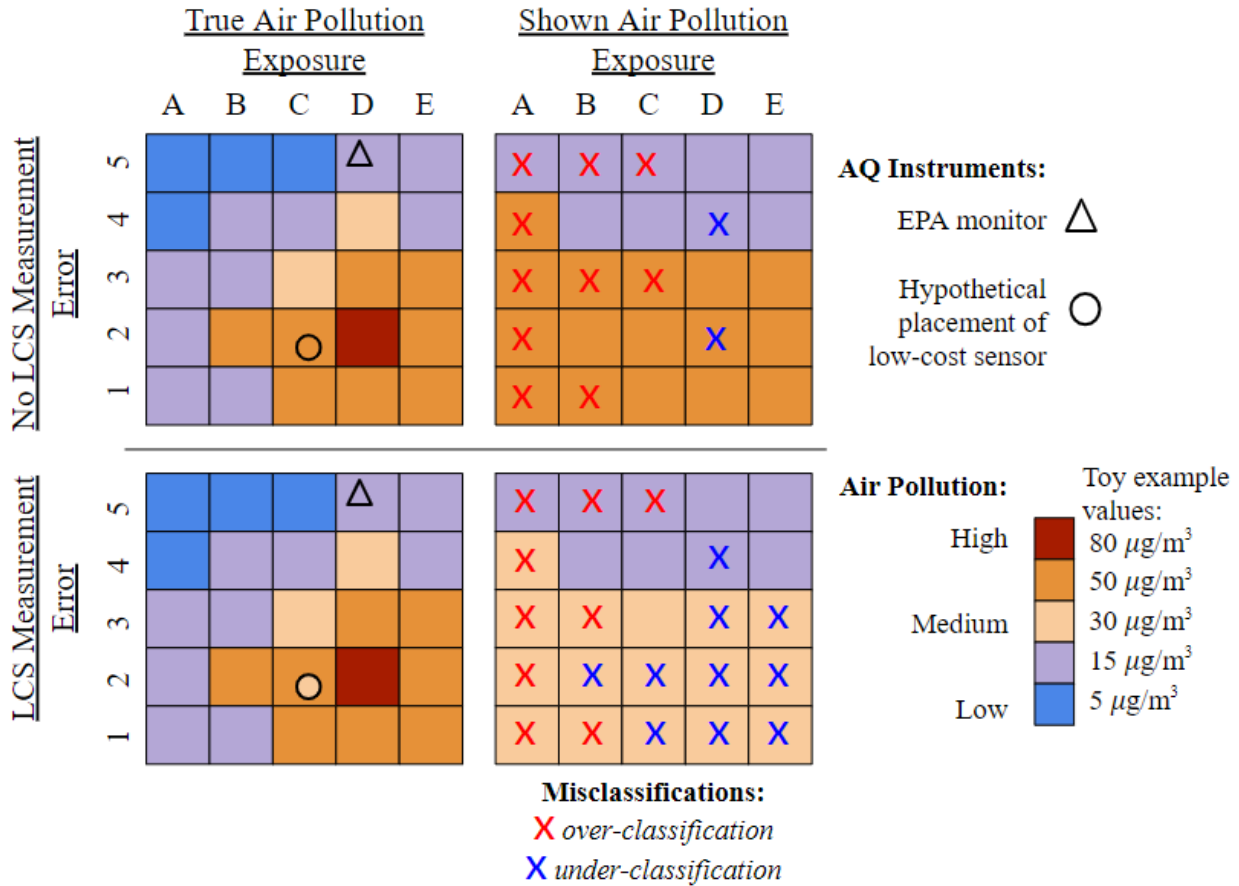


Figure 2: An illustration of the assumed process of AQ information reporting (from each grid’s nearest AQ instrument), under two scenarios: without LCS measurement error (top row of panels) and with LCS measurement error (bottom row of panels). In the True Exposure column, the background color of each grid represents the (unobserved) air quality an individual in that grid experiences, whereas in the Shown Exposure column, the background color represents the air quality an individual in that grid observes from their nearest AQ instrument.

Figure 2 illustrates three distinct sources of AQ reporting error to which we will refer throughout the rest of this paper: (1) distance to the nearest AQ instrument, (2) local variability in air quality, and (3) sensor measurement error. As an example of distance-based errors, the distance between an individual in A5 and the nearest AQ instrument is large, so an individual in A5 is unlikely to be shown accurate measurements of their air pollution exposure (in Figure 2, they would be shown that their exposure is $15 \mu\text{g}/\text{m}^3$ instead of the true exposure, which is $5 \mu\text{g}/\text{m}^3$). As an example of local variability-based errors, while an individual in C5 is close to an EPA monitor (D5), local variability in AQ between C5 and D5 results in misclassification of C5’s AQ (they would be shown that their exposure is $15 \mu\text{g}/\text{m}^3$, while their true exposure is $5 \mu\text{g}/\text{m}^3$). Even if a cell contains an LCS, sensor measurement error may still result in reporting error, as in the case of an individual in C2: under the setting of device measurement error, they would be shown that their exposure is $30 \mu\text{g}/\text{m}^3$, instead of their true exposure, which is $50 \mu\text{g}/\text{m}^3$. These

effects can also co-occur, as for an individual in D2: the nearest AQ instrument is in cell C2, which, in addition to having lower air pollution than D2, also suffers from LCS measurement error. In this paper, we attempt to disentangle these effects.

3.6 Overview: Evaluate the AQ Information

The final step of each simulation is to evaluate the error between the true AQ exposures and the exposures reported by the nearest instrument, summarized across all the grids and days. We evaluate accuracy in AQ reporting using the mean absolute error (MAE) in reported $PM_{2.5}$ concentrations and the misclassification rates of the AQ index, or AQI (34). These metrics are described in the Methods and presented in SI Appendix B.

When calculating these metrics, weighting each grid by its population density allows us to evaluate the accuracy of AQ information available to *individuals* in the California population. We also perform the calculations unweighted by population density, which represents averaging across the land area instead of averaging across individuals. However, as we consider the weighted metrics to be more relevant for public policy (e.g. for health impact assessments), we focus on these results in the main text; the unweighted results are provided in SI Appendix C.

To investigate disparities in AQ information, we compare error for the overall population to error in census block groups in the top quintiles of % poverty and % nonwhite residents, henceforth referred to as Q5 % poverty and Q5 % nonwhite. Maps of % poverty and % nonwhite residents in California are provided in SI Figure A.1.

4. Results

4.1 Descriptive Statistics

Summary statistics of average annual $PM_{2.5}$ (according to the 1km x 1km estimates by Di et al.), % poverty, CES Scores, % nonwhite, and population density, for population subgroups as well as locations (centroids of 1 km x 1 km grid cells) targeted in each of the LCS placement strategies, are shown in SI Table B.1. One key observation, consistent with the environmental justice literature (4–6), is that census block groups (CBGs) with Q5 % poverty or Q5 % nonwhite have higher annual average $PM_{2.5}$ than the population overall. As shown in SI Figure A.2, these marginalized subgroups also experience far more days classified as unhealthy by the AQI (level orange and higher) than the overall population. One differentiator between the two marginalized subgroups (Q5 % nonwhite and Q5 % poverty) is that CBGs with Q5 % nonwhite tend to have higher population density than CBGs with Q5 % poverty.

Another observation from SI Table B.1, consistent with external findings (14), is that among real EPA monitor locations, PurpleAir locations, and the hypothetical LCS placement strategies considered, PurpleAir locations have by far the lowest % poverty. EPA monitor locations have higher % poverty than any of the LCS placement strategies considered. Among the LCS placement strategies considered, schools and locations favored by CES Score have the highest % poverty. LCS placements at schools also have the highest % nonwhite out of any of the EPA monitor, PurpleAir, or hypothetical LCS locations.

Finally, while schools and PurpleAir locations tend to be in CBGs with higher population density, locations chosen to favor proximity to roads, CES Score, and Pollution Score tend to have lower population density.

4.2 Impact of LCS placed at Current PurpleAir Locations on Air Quality Information

The average distance to the nearest EPA monitor is 10.11 km for the population overall, 8.94 km for CBGs with Q5 % nonwhite residents, and 8.69 km for CBGs with Q5 % poverty. When we include LCS at all current locations of outdoor PurpleAir sensors, the average distance to the nearest AQ instrument drops dramatically, to 2.41 km, 2.49 km, and 2.82 km, respectively. Note that these results, like all those in the main text, are weighted by population density. Unweighted results are provided in SI Appendix C.

Table 1 summarizes how the accuracy of daily AQ information changes when we compare the scenario where people only have access to EPA monitors, with the scenario where people have access to EPA monitors *and* LCS at current locations of outdoor PurpleAir sensors. Under the scenario with LCS at PurpleAir locations, we compare the different sensor measurement error types, as described in the Introduction and Methods. The first column of Table 1 shows the amount of sensor measurement error under each type (calculated as the standard deviation of the mean-zero simulated errors). For all the differential sensor measurement error scenarios (10%, 25%, and empirical residual-based), marginalized subgroups on average experience higher sensor measurement error because their air pollution exposure is higher.

Next, we use several metrics to describe the accuracy of observed AQ information under each scenario: (1) absolute error (deviation from the true exposure value), captured using the mean (MAE) and 95th percentile (to illustrate the upper end of the error distribution in addition to the mean), (2) rate of misclassification (either over- or under-classification) of the AQI, and (3) rate of Unhealthy-to-Healthy misclassification (UHM), which we define as the fraction of days with unhealthy AQI that are reported as healthy AQI.

When the LCS have no sensor measurement error (i.e. they are as accurate as EPA monitors in our simulations), deploying them at all the real locations of PurpleAir sensors roughly halves the MAE and 95th percentile of error in daily reported air quality. These improvements are smaller for CBGs with Q5 % poverty, likely because PurpleAir sensors tend to be sited in more socioeconomically privileged areas.

Counterintuitively, even in the absence of sensor measurement error, introduction of the LCS at current PurpleAir locations leads to increases in the rates of under-classification of the AQI and UHMs. These reductions in classification accuracy are likely due to local variability in AQ and PurpleAir locations having lower annual average PM_{2.5} than the state overall (SI Table B.1). This issue is exacerbated by sensor measurement error.

With non-differential sensor measurement error, LCS with error magnitudes of +-10% and +-25% both generally improve on the no-LCS case except for CBGs with Q5 % poverty, where the MAE increases slightly. The impact of sensor measurement error is likely exacerbated for these CBGs with Q5 % poverty due to the socioeconomic bias of PurpleAir locations. By contrast, while 10% differential sensor measurement error improves on the no-LCS case in terms of absolute error, 25% differential error and empirical residual-based error worsen the real-time AQ reporting for all groups and by all metrics, except for small reductions in over-classification of the AQI.

Table 1: Results (weighted by population density) when there are no LCS vs. LCS at all real PurpleAir locations (n = 4,343), assuming different kinds and amounts of sensor measurement error, averaged across 50 simulations to account for randomness in the sensor measurement error generation. Unless otherwise specified, “errors” refer to the difference between the true exposure experienced at each grid centroid and the exposure reported from the nearest AQ instrument. AQI under-classification is when the true exposure class is greater than what someone is shown, and over-classification is when the true exposure class is less than what someone is shown. Rate of UH misclassification (UHM) is the fraction of days with unhealthy AQI (Orange+) that are reported as healthy AQI (Green or Yellow).

Population	Std. Dev. of Sensor Measurement Error ($\mu\text{g}/\text{m}^3$)	MAE ($\mu\text{g}/\text{m}^3$)	95th Percentile of Errors ($\mu\text{g}/\text{m}^3$)	Under-classified AQI (%)	Over-classified AQI (%)	UHM (%)
No LCS (only EPA monitors)						
Overall	—	1.46	4.45	2.05	6.79	11.37
Q5 %	—	1.34	4.14	2.15	6.53	10.35

nonwhite						
Q5 % poverty	—	1.28	4.06	2.09	5.79	8.40
No Sensor Measurement Error						
Overall	0	0.79	2.79	2.12	2.37	15.02
Q5 % nonwhite	0	0.75	2.59	2.22	2.48	13.98
Q5 % poverty	0	0.81	2.80	2.22	2.68	10.06
10% Non-differential Measurement Error						
Overall	0.5	0.94	2.89	2.41	2.80	15.51
Q5 % nonwhite	0.5	0.89	2.71	2.53	2.95	14.58
Q5 % poverty	0.5	0.94	2.90	2.53	3.10	10.34
25% Non-differential Measurement Error						
Overall	1.25	1.33	3.52	3.08	4.12	16.28
Q5 % nonwhite	1.25	1.28	3.39	3.32	4.38	15.56
Q5 % poverty	1.25	1.31	3.52	3.32	4.40	11.36
10% Differential Measurement Error						
Overall	0.88	1.10	3.29	3.19	3.61	20.14
Q5 % nonwhite	0.92	1.08	3.21	3.45	3.84	19.93
Q5 % poverty	0.97	1.13	3.41	3.46	3.90	16.05
25% Differential Measurement Error						
Overall	2.19	1.85	5.39	5.04	6.44	28.68
Q5 % nonwhite	2.30	1.90	5.53	5.66	6.87	28.88
Q5 % poverty	2.44	1.94	5.75	5.78	6.70	25.89

EPA Correction Residual Decile Draws						
Overall	3.32	2.45	7.16	8.28	6.02	27.08
Q5 % nonwhite	3.47	2.51	7.40	9.44	6.32	27.17
Q5 % poverty	3.66	2.54	7.59	9.60	6.15	24.22

The results in this subsection highlight the potential for (i) LCS to reduce both the distance to the nearest AQ instrument and the absolute error in daily PM_{2.5} reporting, (ii) the accuracy of classification-based AQ information to diverge from the accuracy of concentration-based AQ information, (iii) different AQ information outcomes for different subsets of the population, which is related to LCS placement characteristics, and (iv) the dependence of these insights on the type and amount of sensor measurement error.

4.3 Comparing Placement Strategies and Numbers of Sensors Deployed

We now discuss how different hypothetical LCS placement strategies and numbers of LCS deployed affect access to real-time AQ information under both non-differential and differential sensor measurement error conditions.

Figure 3 shows the average distance to the nearest AQ instrument as well as the MAE resulting from simulations under each hypothetical LCS deployment scenario (i.e., each combination of placement strategy and number of LCS deployed) and for each sensor measurement error type. The vertical scales of each plot are different, to facilitate close inspection of the lines. The plot for 10% non-differential measurement error is not shown because it is very similar to panel b.

The six panels in Figure 3 help distinguish between the three different components of error in real-time AQ reporting. First, we observe that with zero or low amounts of LCS measurement error, much of the average error in daily AQ reporting is due to individuals' distance to the nearest AQ instrument, as illustrated by the similarity in line ordering and slopes between panels a, b, and d. Another observation, however, is that the impact of reduction in distance to the nearest AQ instrument can be confounded by local variability in AQ. For example, while LCS placements favoring CBGs with high Pollution Score result in greater reduction in distance to the nearest AQ instrument than placements favoring CBGs with high CES Score (panel a), the CES Score placement strategy results in lower MAE (panel b). This phenomenon is explained by local variability in AQ because the Pollution Score primarily highlights areas with large local sources of pollution, so measurements in those pollution “hotspots” may not be representative of air pollution even in nearby communities.

For low amounts of sensor measurement error (i.e. 10% non-differential and differential, as shown in panel d), reductions in daily AQ reporting error due to decreased distance to the nearest AQ instrument mitigate the impact of the LCS measurement error, improving MAEs across the board. When sensor measurement error is increased to 25% non-differential (panel c), deploying LCS only improves MAE under certain placement strategies: at schools and in current PurpleAir locations. This is because these placement strategies prioritize areas with higher population density.

With 25% differential and empirical residual-based sensor measurement errors (panels e and f), the impact of reduced distance to the nearest AQ instrument is overshadowed by the increased error in the sensor measurements, worsening AQ reporting across the board. Under these large amounts of sensor measurement error, placements favoring high CES Score result in the least error in AQ reporting. In nearly all cases, marginalized subgroups experience lower MAE than the population overall.

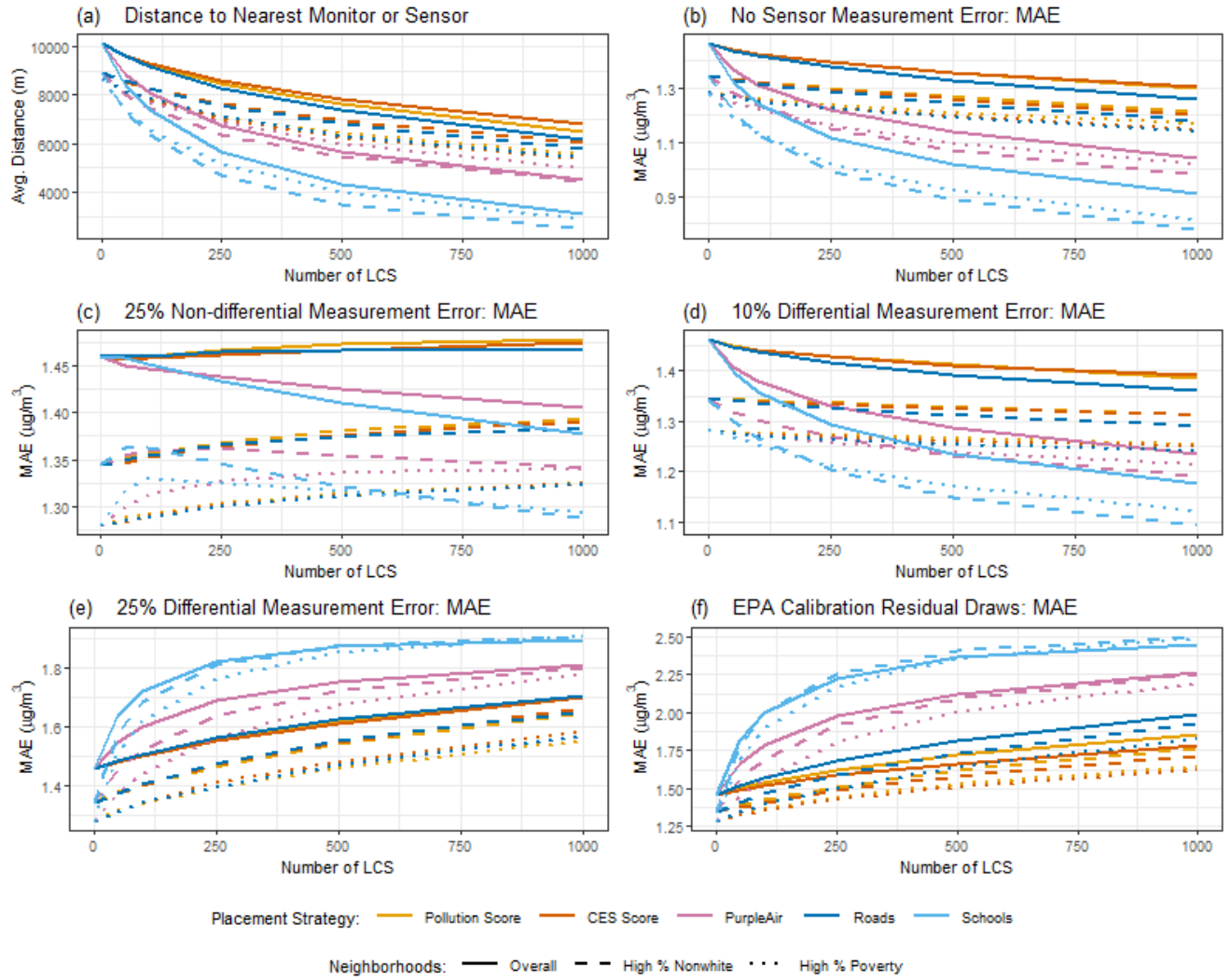


Figure 3: Distance to the nearest AQ instrument and mean absolute error (between what is reported vs. experienced) resulting from different numbers of LCS deployed, LCS placement strategies, and sensor measurement error types and amounts. All results were calculated using 366 days and averaged across 50 simulation trials, weighted by population density.

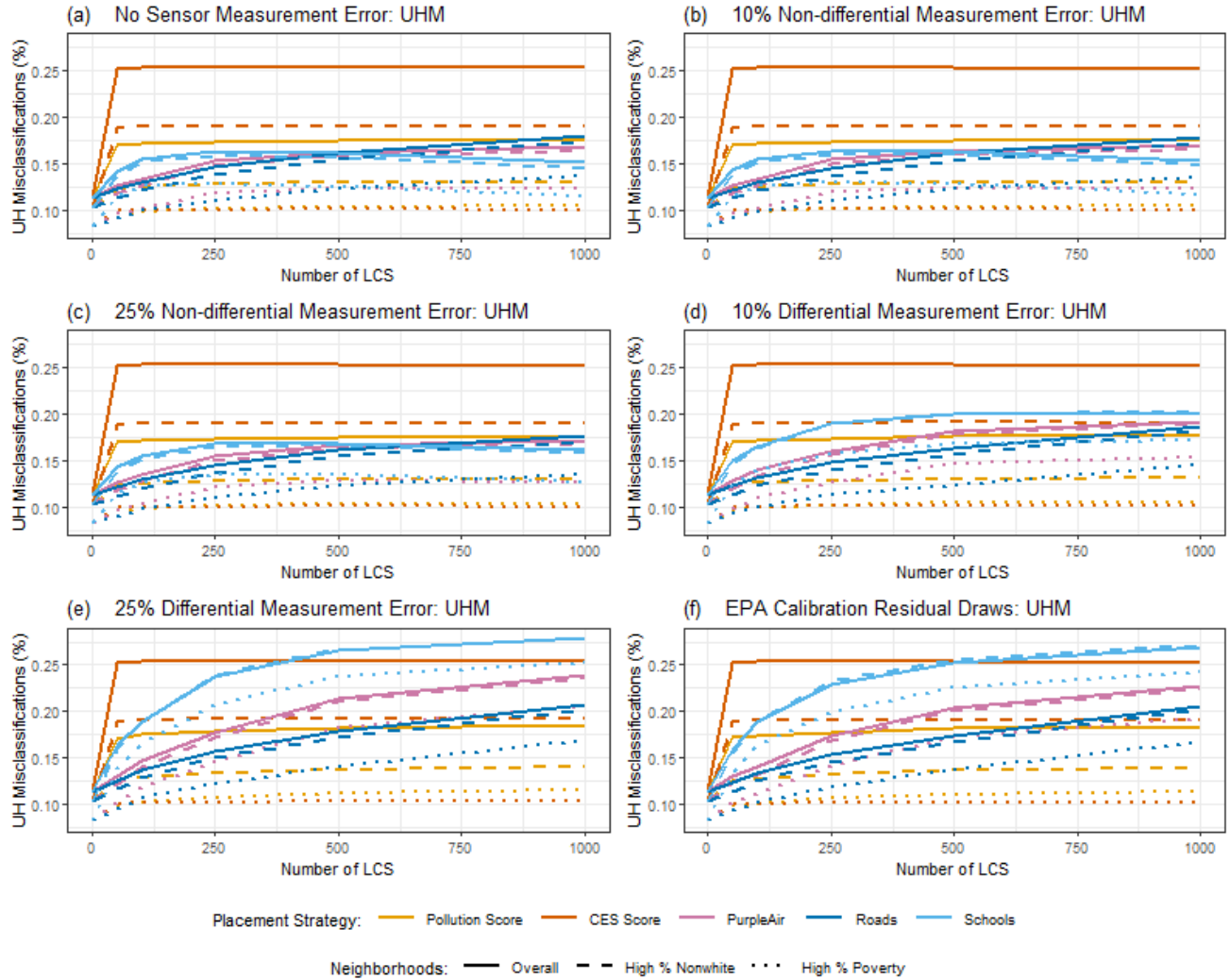


Figure 4: Rates of UH misclassification resulting from different numbers of LCS deployed, LCS placement strategies, and sensor measurement error types and amounts. UH misclassification occurs when the AQ is unhealthy (Orange+) but is reported as healthy (Green or Yellow); the UHM rate is calculated by dividing the fraction of UH misclassifications by the total fraction of unhealthy days experienced by each group. All results were calculated using 366 days and averaged across 50 simulation trials, weighted by population density.

Figure 4 shows the rate of UH misclassifications (UHMs) for all placement strategies, numbers of LCS deployed, and sensor measurement error types and amounts. One of the most noticeable patterns from Figure 4 is how the rate of UHMs increases when any LCS are introduced under all placement strategies. This is especially true for LCS placements based on CES Score and Pollution Score (for the population overall and CBGs with Q5 % nonwhite): the UHM rates stay basically constant despite the changing number of LCS. We posit that this is due to high local variability in AQ in Census tracts with high Pollution or CES Scores.

Another important observation is that although marginalized subgroups experience a higher number of unhealthy days in absolute terms, the fraction of those unhealthy days misclassified as healthy is lower than for the population overall. And, crucially, the CES and Pollution Score-based placements lead to the lowest UHM rates for CBGs with Q5 % poverty. However, school locations are the only placement strategy resulting in decreasing UHMs for large numbers of LCS deployed (when sensor measurement error is low, in panels a through c), so it is possible that school placement strategies may eventually lead to the lowest rate of UHMs, as more LCS are deployed.

Finally, although generally increasing sensor measurement error increases the rate of UHMs, the empirical residual-based errors (panel f) result in slightly lower UHMs than the 25% differential scenario (in panel e) for LCS at schools and PurpleAir locations.

Further disentanglement of the contributions of distance, local variability in AQ, and sensor measurement error to large misclassifications of the AQI (off by more than one class), for each of the LCS placement strategies, is provided in the Supplemental Results.

5. Discussion

5.1 Conclusions

In this study, we investigated the utility of including measurements from LCS in real-time AQ reporting using simulations based closely on real data. By comparing different types and amounts of sensor measurement error as well as different LCS placement strategies and numbers of LCS deployed, we were able to differentiate between the impacts of three components of error in daily AQ reporting: distance to the nearest AQ instrument, local variability in air quality, and sensor measurement error.

Our findings offer several key insights and suggestions. One of the most important is that the value of using LCS for real-time AQ reporting depends strongly on the amount and type of sensor measurement error, and also on the metric to which people pay attention (i.e. absolute concentration vs. AQI classification). Considering MAE, deploying LCS with 10% measurement error (differential or non-differential) improves daily AQ reporting (compared to only using EPA monitors) across the board. However, among the placement strategies considered here, only LCS placements at schools and PurpleAir locations improve AQ reporting when sensor measurement error is 25% non-differential. Deploying LCS with 25% differential measurement error worsens daily AQ reporting across the board.

By contrast, introducing any number of LCS with any amount of sensor measurement error increases the rate of UH misclassifications, which may be even more relevant than absolute

PM_{2.5} concentrations for public health. However, beyond 500 LCS deployed, the UHM rate decreases again for placements at schools when sensor measurement error is 10% or 25% non-differential, so this issue might be mitigated with large numbers of LCS.

Accounting for both absolute concentration and AQI classification metrics, it appears that placing LCS at schools results in the most accurate and equitable distribution of daily AQ information when sensor measurement error is less than 25% nondifferential and more than 500 LCS are deployed. The latter is quite realistic given that in California in 2021, there were 4,343 1 km x 1 km grids with PurpleAir, not to mention other brands of LCS. From a health standpoint, children's relatively high vulnerability to air pollution (35) further motivates the strategy of placing LCS at schools.

For our empirically-based simulation, the degree of error injected into our simulated LCS measurements was drawn from the empirical distribution of errors between collocated California EPA monitor and PurpleAir sensor data after correction using a national equation developed by EPA researchers (33). This degree of measurement error is believed to most closely reflect error in the publicly available LCS measurements available through many programs and platforms today. Our simulations show that, under these conditions, using data from LCS in real-time AQ reporting would worsen the accuracy of information from people's nearest AQ instrument, both on average and for the marginalized groups considered. This result suggests that more region-specific LCS calibration procedures may be necessary for this application of LCS, which aligns with the findings of several recent studies advocating for region-specific corrections (20, 36).

When sensor measurement error is high, LCS placement strategies that prioritize those burdened by environmental pollution and sociodemographics result in the most equitable provision of AQ information. Also, across all levels of sensor measurement error and numbers of LCS deployed, selecting LCS placements based on CES Score results in the lowest rate of UHMs for CBGs with Q5 % poverty. Lastly, our simulations revealed that the CES and Pollution Score-based placements are often affected by high local variability in air quality, which makes sense because they tend to be near major sources of air pollution. These results indicate that while placing LCS in environmental justice hotspots may benefit those in the immediate community, integrating their data into wider AQ reporting platforms may lead to worsening of real-time AQ information for those outside the immediate community.

Balancing policy priorities related to LCS deployment will not be easy. To balance the needs of people in less densely populated communities with those of people in more densely populated communities, our analysis unweighted by population density (results shown in SI Appendix C) suggests that some strategic deployments near major roads (especially in less densely populated areas) might also be beneficial.

These results can inform future investment in LCS networks for equitable AQ monitoring programs in the US, and the methods used can inform similar studies in other locales. While our findings are based on PurpleAir sensors for PM_{2.5}, this work informs accuracy targets and larger concerns about LCS placement and calibration across brands of PM_{2.5} sensors, and possibly for other air pollutants. However, we reiterate that this analysis has focused on the use of LCS for provision of real-time AQ information to the public. These insights do not necessarily transfer to other applications. For example, in longer-term applications, LCS have been shown to help capture neighborhood-scale PM_{2.5} when fused with satellite data (37) or incorporated into either a kriging model (38–40) or a machine learning model with spatially-varying correction for the LCS (23).

5.2 Limitations and Future Directions

Design-related limitations of our study are that we only used data from California and that we assumed individuals only view the AQ information from the instrument nearest to their location of residence. A technical limitation of this analysis is our use of the Di et al. daily 1 km x 1 km estimates for the “true” exposures. AQ may vary substantially over 24 hours and over a 1 km x 1 km square, and as several studies have observed, the PM_{2.5} patterns sensed by LCS are often different (i.e. affected more by local sources) than EPA monitors (41, 42), which Di et al. used to train their model. We also did not consider any differences in LCS performance due to varying PM composition, which have been observed elsewhere (32).

Future work might consider more nuance in the LCS measurement error problem, such as accounting for sensor “drift” (19, 43, 44) and varying particle composition / meteorological conditions, as has been explored by EPA researchers who have proposed a different correction method for wildfire smoke measured by PurpleAir sensors (45). In terms of LCS placement, while we chose relatively simple selection strategies to facilitate comprehension and comparison, future research could harness more sophisticated statistical and/or atmospheric modeling techniques (39, 46, 47) to identify locations yielding key spatiotemporal information or to prioritize some LCS placements near EPA monitors for the purposes of sensor calibration. Finally, there is more work to be done investigating how access to real-time AQ information and/or alerts translates into public health and economic benefits, as several studies have begun exploring (48–52).

6. Materials & Methods

In this analysis, we compared several different types and amounts of sensor measurement error for five different placement strategies of LCS: at current outdoor PurpleAir locations, at public schools, in locations favoring proximity to major roads, and in locations favoring proximity to

environmentally and socioeconomically marginalized communities. The LCS placement strategies, sensor measurement error simulation methods, and full simulation procedure are described in detail in the following subsections.

6.1 LCS Placement Strategies and Data Sources

Table 2 describes the data sets, data processing steps, and sampling methods used to select locations for LCS in each simulation.

We note that CES Scores are a product of environmental and socioeconomic-demographic indices. The environmental disadvantage index, referred to in this paper as Pollution Score, incorporates data on air pollution (ozone, PM_{2.5}, diesel PM emissions, toxic chemical releases from facilities) and traffic density; pesticides, groundwater threats, impaired water bodies, and drinking water contamination index; solid waste, hazardous waste, and cleanup sites. The correlation between the Pollution Scores and the PM_{2.5} estimates from Di et al. is 0.48. The socioeconomic-demographic (population) disadvantage index incorporates data on asthma, low birth weight, cardiovascular disease, education, linguistic isolation, poverty, unemployment, and housing burden.

Table 2: Describing the data sets, data processing steps, and sampling methods used to select locations for LCS in each simulation.

Placement strategy	Data source	Data processing	LCS location selection method (within each simulation)	Additional notes
Current PurpleAir Locations	The purpleair Python package (53)	Assigned each outdoor PurpleAir sensor to its nearest 1 km x 1 km grid centroid	Randomly selected grids with PurpleAir	4,343 grids with PurpleAir LCS
Public School Locations	The National Center for Education Statistics (54)	Assigned each school to its nearest 1 km x 1 km grid centroid	Randomly selected grids with schools	7,548 grids with schools
Near-Road	The National Highway Planning Network shapefile (55)	Summed the lengths of major roads within circular buffers with 500 m radii around each grid centroid	Randomly sampled from all grids, where the sampling probability for each grid was the sum of road lengths	4.5% of the grids had major roads; among these, the average length was

				2km
CES Score	Cal Enviro Screen 3.0 (31)	Assigned all grids the CES Score of the census tract their centroid falls within	Randomly sampled from all grids, where the sampling probability for each grid was the CES Score	<i>Additional notes are in the main text</i>
Pollution Score	Cal Enviro Screen 3.0 (31)	Assigned all grids the Pollution Score of the census tract their centroid falls within	Randomly sampled from all grids, where the sampling probability for each grid was the Pollution Score	<i>Additional notes are in the main text</i>

We also obtained socio-demographic features from the 2016 American Community Survey (56) using the R package tidycensus (57), at the finest spatial resolution for which they were available: Census block group (CBG) level for race/ethnicity and population density, and Census tract level for socioeconomic status. To merge these features with the AQ data, we performed an overlay of the Census shapefile with the 1 km x 1 km grid centroids from the Di et al. estimates. Any block group or tract that did not contain a grid centroid was ignored.

For this analysis, we used percentage of non-white individuals (all but non-Hispanic white) for the percent marginalized by race/ethnicity and the percent of people living under the poverty line for those marginalized by socioeconomic status. Our decision to use one minus the percent of non-Hispanic white people to represent disadvantage by race/ethnicity (elsewhere referred to as “% nonwhite” for verbal simplicity) was informed by a preliminary calculation showing that Hispanic white people on average experience higher pollution and socioeconomic disadvantage than the overall white population. We defined CBGs with high % nonwhite and high % poverty to be CBGs that fell into the top quintiles of these measures in California ($\geq 58.1\%$ and $\geq 23.5\%$ respectively). For the 0.3% of CBGs that were missing data on % nonwhite, we substituted in Census tract-level % nonwhite. Only for one tract with population > 0 (tract 6037920200 with population 5,000), were we unable to retrieve tract-level data, and thus we omitted this tract from the analysis.

6.2 Measurement Error Simulation

6.2.1 Sampling from the Empirical Distribution of PurpleAir Errors

To obtain a realistic distribution of measurement errors for our simulated LCS, we compared PurpleAir measurements and EPA monitor measurements for collocated EPA monitor and LCS pairs in California. We obtained daily PM_{2.5} averages for both of these sources from the year 2020 (as opposed to 2016, the year for which we had 1 km x 1 km estimates from Di et al. to use

as “truth” in the simulations) because most of the PurpleAir sensors have been deployed since 2016. We used the purpleair Python package to obtain measurements of PM_{2.5}, temperature, and relative humidity from PurpleAir sensors (channel A on 1/11/22 and channel B on 1/23/22), and downloaded the EPA monitor measurements from the EPA Air Quality System annual summary files repository (58).

Following the 24-hour quality assurance methods of the EPA researchers who developed a national correction for PurpleAir data (33), we identified all pairs of EPA monitors and outdoor PurpleAir sensors within 50 meters of each other. Then, also following their quality assurance methods, we only considered EPA monitor averages based on at least 18 hours of observation, and PurpleAir averages based on at least 90% of the 2-minute observations, where the difference in daily averages of the two PurpleAir channels was less than 5 μg/m³ or 61%. Then, we averaged the PurpleAir channels. This procedure yielded 5,759 paired daily observations from 22 EPA monitor-PurpleAir locations. To make this distribution more realistic for 2016, we removed 48 daily observations where the EPA monitor PM_{2.5} was greater than 112 μg/m³ (the maximum value in the 2016 Di et al. estimates), yielding n = 5,711.

The EPA correction equation developed for PurpleAir sensors in the US is
$$PM_{2.5} = 0.524 \times \{\text{PurpleAir } PM_{2.5}\} - 0.0862 \times \{\text{Relative Humidity}\} + 5.75$$

After applying this correction to the PurpleAir data, we compared the corrected values to the collocated EPA monitor measurements. The resulting RMSE (root-mean squared error) was 5.33 μg/m³ and R² was 0.81. We refer to the difference between these EPA monitor and corrected LCS measurements as the empirical residuals.

SI Figure A.3 shows that the magnitude of empirical residuals increased as the true PM_{2.5} concentration (as measured by the EPA monitors) increased. Sensor measurement error increasing with PM_{2.5} concentration (i.e., differential measurement error) has been observed by some other groups as well (15). Such a relationship was not observed for relative humidity nor ambient temperature. Thus, for the empirically-based LCS measurement error simulation, we sampled from the distribution of residuals corresponding to the decile of true PM_{2.5} (the Di et al. estimates) at each grid and day. A summary of the Di et al. estimates mapped into these deciles is given in SI Table A.2.

6.2.2 Fully Synthetic LCS Errors Based on Proposed Performance Targets

To further investigate the effect of sensor measurement error, we also ran simulations using no sensor measurement error (as if the LCS were as accurate as the EPA monitors) and two different amounts of both non-differential and differential sensor measurement error. For a given accuracy level (either ±10% or ±25%, as proposed in the EPA performance targets workshop (32)), we

simulated non-differential sensor measurement error by sampling from a normal distribution with mean zero and standard deviation of 5 (the unweighted 2016 average PM_{2.5} in California) multiplied by the accuracy level, yielding 0.5 and 1.25 respectively. In mathematical notation:

$$\{\text{LCS PM}_{2.5}\} = \{\text{Di et al. PM}_{2.5}\} + \varepsilon_n$$

where $\varepsilon_n \sim \text{Normal}(\text{mean} = 0, \text{sd} = \{0.1 \text{ or } 0.25\} * 5)$

The differential sensor measurement error, on the other hand, was motivated by our observation of the positive correlation between the magnitude of the EPA correction residuals and the true PM_{2.5}. For the two accuracy levels, we simulated differential sensor measurement error by sampling from a normal distribution with mean zero and standard deviation of the true PM_{2.5} (for each grid and day) multiplied by the accuracy level. In mathematical notation:

$$\{\text{LCS PM}_{2.5}\} = \{\text{Di et al. PM}_{2.5}\} + \varepsilon_d$$

where $\varepsilon_d \sim \text{Normal}(\text{mean} = 0, \text{sd} = \{0.1 \text{ or } 0.25\} * \{\text{Di et al. PM}_{2.5}\})$

Comparison of the characteristics and effects of these different types and amounts of sensor measurement error is facilitated by Table 1 in section 4.2.

6.3 Simulation Procedure

For each combination of placement strategy and sensor measurement error, we ran five experiments, using 0, 50, 100, 250, 500, and 1000 LCS to show the trends. Additionally, we ran an experiment for each type and amount of sensor measurement error with LCS at all the real locations of outdoor PurpleAir ($n = 4,343$ grid cells). For each experiment, we ran 50 trials and averaged across them to account for random sampling variability. Comparison across several numbers of trials and inspection of the resulting plots indicates that 50 trials is sufficient for this purpose. In all of these simulations, for each trial, we randomly sampled LCS locations according to the given strategy, and simulated the LCS PM_{2.5} measurements by adding measurement error to the “true” PM_{2.5} (from Di et al estimates) at the selected LCS locations for each day. For every day in 2016, we assigned every 1 km x 1 km grid in California the AQ “measurement” from the nearest AQ instrument (EPA monitor or LCS), representing the AQ information that individuals living in each grid are shown (e.g., by a smartphone app).

We then calculated metrics to evaluate the accuracy of people’s daily AQ information, averaging across all days in 2016 and all grids in California. In the next subsection, we describe how we also ran subset calculations for grids within marginalized CBGs. We refer to the difference between the AQ people observe (from the nearest AQ instrument) and their true AQ exposure as the reporting error. The evaluation metrics we used fall into three categories: error-based metrics,

misclassification metrics, and proximity metrics. The error-based metrics are mean absolute error (MAE) and 95th percentile of errors.

The misclassification metrics rely on the U.S. Air Quality Index, or AQI (34). The AQI classifies AQ into six levels, with different public health recommendations for each. Green = “Good”, Yellow = “Moderate”, Orange = “Unhealthy for Sensitive Groups”, Red = “Unhealthy”, Purple = “Very Unhealthy”, and Maroon = “Hazardous”. AQI is often reported as a combination of air pollutants, however, for this analysis we use the single-pollutant version for PM_{2.5} (59). We hypothesize that most people use these classifications to inform their activity rather than the exact concentrations of PM_{2.5} (or any other air pollutant), so we calculated the percent of over- and under-classifications, the percent of misclassifications greater than one level (e.g. Orange → Green or Yellow → Red), and what we term UH misclassifications: the fraction of days that a healthy (H) classification is shown, out of the days that are truly unhealthy (U). This last metric may be of the most concern for public health. For this dichotomous variable, we defined Green and Yellow to be healthy, and Orange through Maroon to be unhealthy.

The proximity metrics can be used to investigate the mechanisms behind the other results, specifically the effects of additional measurement error and shorter distances to the nearest sensor as we “deploy” more LCS. To get at these factors, we calculate the mean distance to the nearest AQ instrument, overall as well as among instances that were misclassified in the AQI.

6.4 Evaluating Equity Across Individuals and Groups

In addition to the overall population metrics (averaging across all grids in California), we calculated the metrics (described in subsection 6.3) for marginalized subsets of the population, to determine if certain sensor placement strategies resulted in more equitable or less equitable access to AQ information. Specifically, we considered CBGs with high percent of nonwhite residents and CBGs with high percent of residents living below the poverty line.

Finally, for all metrics, we calculate versions weighted and unweighted by population density. Weighting by the population density at each grid point (obtained via spatial overlay as described above) assigns equal importance to each individual’s AQ information, whereas the unweighted version assigns equal importance across the land area. Thus, the weighted results are more relevant for urban areas, while the unweighted results are more relevant for rural areas.

6.5 Software Availability

Code used to process the datasets, run the analyses and generate the figures and tables can be found at https://github.com/EllenConside/LCS_placement_sims

7. Acknowledgments and Funding Sources

This work was supported by NIH grant 5T32ES007142 (the Harvard Biostatistics Department) and NIH grant 1K01ES032458. We would also like to thank the National Studies on Air Pollution and Health (NSAPH) research lab, specifically the biostatistics working group led by Francesca Dominici, for their support.

8. Author Contributions

- Ellen Considine: conceptualization, data analysis, results visualization, writing and editing
- Danielle Braun, Rachel Nethery, and Priyanka deSouza: conceptualization, writing and editing
- Leila Kamareddine: writing and editing

9. References

1. Q. Di, *et al.*, Association of Short-Term Exposure to Air Pollution with Mortality in Older Adults. *JAMA* **318**, 2446–2456 (2017).
2. Q. Di, *et al.*, Air Pollution and Mortality in the Medicare Population. *N. Engl. J. Med.* **376**, 2513–2522 (2017).
3. US EPA, How Does PM Affect Human Health? | Air Quality Planning Unit | Ground-level Ozone | New England | US EPA (May 6, 2022).
4. A. Jbaily, *et al.*, Air pollution exposure disparities across US population and income groups. *Nature* **601**, 228–233 (2022).
5. J. Colmer, I. Hardman, J. Shimshack, J. Voorheis, Disparities in PM_{2.5} air pollution in the United States. *Science* **369**, 575–578 (2020).
6. C. W. Tessum, *et al.*, Inequity in consumption of goods and services adds to racial–ethnic disparities in air pollution exposure. *Proc. Natl. Acad. Sci.* **116**, 6001–6006 (2019).
7. H. Orru, K. L. Ebi, B. Forsberg, The Interplay of Climate Change and Air Pollution on Health. *Curr. Environ. Health Rep.* **4**, 504–513 (2017).
8. D. Miller, A Low-cost Air Quality Sensor for Measuring Particulate Matter (U.S. National Park Service). *Intermt. Park Sci. II* (November 14, 2021).
9. J. P. Keller, R. D. Peng, Error in estimating area-level air pollution exposures for epidemiology. *Environmetrics* **30** (2019).

10. P. B. English, *et al.*, The Imperial County Community Air Monitoring Network: A Model for Community-based Environmental Monitoring for Public Health Action. *Environ. Health Perspect.* **125**, 074501 (2017).
11. C. Grainger, A. Schreiber, Discrimination in Ambient Air Pollution Monitoring? *AEA Pap. Proc.* **109**, 277–282 (2019).
12. J. G. Watson, J. C. Chow, D. DuBois, M. Green, N. Frank, “Guidance for the network design and optimum site exposure for PM_{2.5} and PM₁₀” (Environmental Protection Agency, Office of Air Quality Planning and Standards, Research Triangle Park, NC (United States); Nevada Univ. System, Desert Research Inst., Reno, NV (United States); National Oceanic and Atmospheric Administration, Las Vegas, NV (United States), 1997) (January 3, 2022).
13. US EPA, How to Use Air Sensors: Air Sensor Guidebook (2016) (November 14, 2021). <https://www.epa.gov/air-sensor-toolbox/how-use-air-sensors-air-sensor-guidebook>
14. P. deSouza, P. L. Kinney, On the distribution of low-cost PM_{2.5} sensors in the US: demographic and air quality associations. *J. Expo. Sci. Environ. Epidemiol.* **31**, 514–524 (2021).
15. Y. Lu, G. Giuliano, R. Habre, Estimating hourly PM_{2.5} concentrations at the neighborhood scale using a low-cost air sensor network: A Los Angeles case study. *Environ. Res.* **195**, 110653 (2021).
16. R. Jayaratne, *et al.*, Low-cost PM_{2.5} Sensors: An Assessment of Their Suitability for Various Applications. *Aerosol Air Qual. Res.* (2020) <https://doi.org/10.4209/aaqr.2018.10.0390> (January 27, 2022).
17. L. R. Crilley, *et al.*, Effect of aerosol composition on the performance of low-cost optical particle counter correction factors. *Atmospheric Meas. Tech.* **13**, 1181–1193 (2020).
18. X. Liu, *et al.*, Low-cost sensors as an alternative for long-term air quality monitoring. *Environ. Res.* **185**, 109438 (2020).
19. E. M. Considine, C. E. Reid, M. R. Ogletree, T. Dye, Improving accuracy of air pollution exposure measurements: Statistical correction of a municipal low-cost airborne particulate matter sensor network. *Environ. Pollut.* **268**, 115833 (2021).
20. M. Zusman, *et al.*, Calibration of low-cost particulate matter sensors: Model development for a multi-city epidemiological study. *Environ. Int.* **134**, 105329 (2020).
21. C. Malings, *et al.*, Fine particle mass monitoring with low-cost sensors: Corrections and long-term performance evaluation. *Aerosol Sci. Technol.* **54**, 160–174 (2020).

22. C. Heffernan, R. Peng, D. R. Gentner, K. Koehler, A. Datta, Gaussian Process filtering for calibration of low-cost air-pollution sensor network data. *ArXiv220314775 Stat* (2022) (May 6, 2022).
23. J. Bi, *et al.*, Contribution of low-cost sensor measurements to the prediction of PM_{2.5} levels: A case study in Imperial County, California, USA. *Environ. Res.* **180**, 108810 (2020).
24. L. Morawska, *et al.*, Applications of low-cost sensing technologies for air quality monitoring and exposure assessment: How far have they gone? *Environ. Int.* **116**, 286–299 (2018).
25. Clarity: A Guide to Leveraging Low-Cost Sensors for Air Quality Monitoring (2021) (January 27, 2022). <https://www.clarity.io/landing-pages/download-guide>
26. M. Burke, *et al.*, The changing risk and burden of wildfire in the United States. *Proc. Natl. Acad. Sci.* **118**, e2011048118 (2021).
27. M. Goss, *et al.*, Climate change is increasing the likelihood of extreme autumn wildfire conditions across California. *Environ. Res. Lett.* **15**, 094016 (2020).
28. P. Gupta, *et al.*, Impact of California Fires on Local and Regional Air Quality: The Role of a Low-Cost Sensor Network and Satellite Observations. *GeoHealth* **2**, 172–181 (2018).
29. J. C. Liu, *et al.*, Wildfire-specific Fine Particulate Matter and Risk of Hospital Admissions in Urban and Rural Counties: *Epidemiology* **28**, 77–85 (2017).
30. Q. Di, An ensemble-based model of PM_{2.5} concentration across the contiguous United States with high spatiotemporal resolution. *Environ. Int.*, 13 (2019).
31. California Office of Environmental Health Hazard Assessment, CalEnviroScreen 3.0. (2016) (November 6, 2021). <https://oehha.ca.gov/calenviroscreen/report/calenviroscreen-30>
32. R. Williams, *et al.*, Deliberating performance targets workshop: Potential paths for emerging PM_{2.5} and O₃ air sensor progress. *Atmospheric Environ. X* **2**, 100031 (2019).
33. K. K. Barkjohn, B. Gantt, A. L. Clements, Development and application of a United States-wide correction for PM_{2.5} data collected with the PurpleAir sensor. *Atmospheric Meas. Tech.* **14**, 4617–4637 (2021).
34. AQI Basics | AirNow.gov (November 6, 2021). <https://www.airnow.gov/aqi/aqi-basics/>
35. European Center for Environment and Health, Bonn Office. *Effect of Air Pollution on Children's Health and Development: A Review of the Evidence* (2005).

36. H.-J. Chu, M. Z. Ali, Y.-C. He, Spatial calibration and PM_{2.5} mapping of low-cost air quality sensors. *Sci. Rep.* **10**, 22079 (2020).
37. K. Huang, *et al.*, Estimating daily PM_{2.5} concentrations in New York City at the neighborhood-scale: Implications for integrating non-regulatory measurements. *Sci. Total Environ.* **697**, 134094 (2019).
38. T. Lu, M. J. Bechle, Y. Wan, A. A. Presto, S. Hankey, Using crowd-sourced low-cost sensors in a land use regression of PM_{2.5} in 6 US cities. *Air Qual. Atmosphere Health* **15**, 667–678 (2022).
39. J. Bi, *et al.*, Publicly available low-cost sensor measurements for PM_{2.5} exposure modeling: Guidance for monitor deployment and data selection. *Environ. Int.* **158**, 106897 (2022).
40. A. Gressent, L. Malherbe, A. Colette, H. Rollin, R. Scimia, Data fusion for air quality mapping using low-cost sensor observations: Feasibility and added-value. *Environ. Int.* **143**, 105965 (2020).
41. W.-C. V. Wang, S.-C. C. Lung, C.-H. Liu, Application of Machine Learning for the in-field Correction of a PM_{2.5} Low-Cost Sensor Network. *Sensors* **20**, 5002 (2020).
42. R. Tanzer, C. Malings, A. Haurlyliuk, R. Subramanian, A. A. Presto, Demonstration of a Low-Cost Multi-Pollutant Network to Quantify Intra-Urban Spatial Variations in Air Pollutant Source Impacts and to Evaluate Environmental Justice. *Int. J. Environ. Res. Public Health* **16**, 2523 (2019).
43. F. Delaine, B. Lebental, H. Rivano, *In Situ* Calibration Algorithms for Environmental Sensor Networks: A Review. *IEEE Sens. J.* **19**, 5968–5978 (2019).
44. C. Malings, *et al.*, Development of a general calibration model and long-term performance evaluation of low-cost sensors for air pollutant gas monitoring. *Atmospheric Meas. Tech.* **12**, 903–920 (2019).
45. K. Johnson, A. Holder, S. Frederick, A. Clements, “PurpleAir PM_{2.5} U.S. Correction and Performance During Smoke Events” (EPA, 2020) (November 6, 2021).
46. M. Kelp, S. Lin, J. N. Kutz, L. J. Mickley, A new approach for determining optimal placement of PM_{2.5} air quality sensors: case study for the contiguous United States. *ArXiv171200642 Stat* (2022) (January 24, 2022).
47. P. J. Diggle, E. Giorgi, Preferential sampling of exposure levels. *J A*, 14 (2019).

48. D. D'Antoni, *et al.*, The effect of evidence and theory-based health advice accompanying smartphone air quality alerts on adherence to preventative recommendations during poor air quality days: A randomised controlled trial. *Environ. Int.* **124**, 216–235 (2019).
49. S. Saberian, A. Heyes, N. Rivers, Alerts work! Air quality warnings and cycling. *Resour. Energy Econ.* **49**, 165–185 (2017).
50. X.-J. Wen, L. Balluz, A. Mokdad, Association Between Media Alerts of Air Quality Index and Change of Outdoor Activity Among Adult Asthma in Six States, BRFSS, 2005. *J. Community Health* **34**, 40–46 (2009).
51. M. Neidell, P. L. Kinney, Estimates of the association between ozone and asthma hospitalizations that account for behavioral responses to air quality information. *Environ. Sci. Policy* **13**, 97–103 (2010).
52. J. J. Buonocore, L. A. Robinson, J. K. Hammitt, L. O'Keeffe, Estimating the Potential Health Benefits of Air Quality Warnings. *Risk Anal.* **41**, 645–660 (2021).
53. C. Sardegna, *purpleair package*. https://github.com/ReagentX/purple_air_api
54. School Locations & Geoassignments 2020-2021, Education Demographic and Geographic Estimates | National Center for Education Statistics (November 6, 2021). <https://nces.ed.gov/programs/edge/geographic/schoollocations>
55. National Highway Planning Network | U.S. D.O.T. Federal Highway Administration (November 6, 2021). <https://www.fhwa.dot.gov/planning/processes/tools/nhpn/>
56. A. C. S. O. | U. C. Bureau, Data Profiles. *U. S. Census Bur.* (January 27, 2022).
57. K. Walker, *tidycensus*. <https://walker-data.com/tidycensus/>
58. EPA AirData website file download page (November 14, 2021). https://aqs.epa.gov/aqsweb/airdata/download_files.html#Daily
59. The AQI Equation - Air Quality and AQI Info. *AirNow Discuss. Forum* (2016) (November 6, 2021). <https://forum.airnowtech.org/t/the-aqi-equation/169>

Supplemental Information for “Investigating Use of Low-Cost Sensors to Increase Accuracy and Equity of Real-Time Air Quality Information”

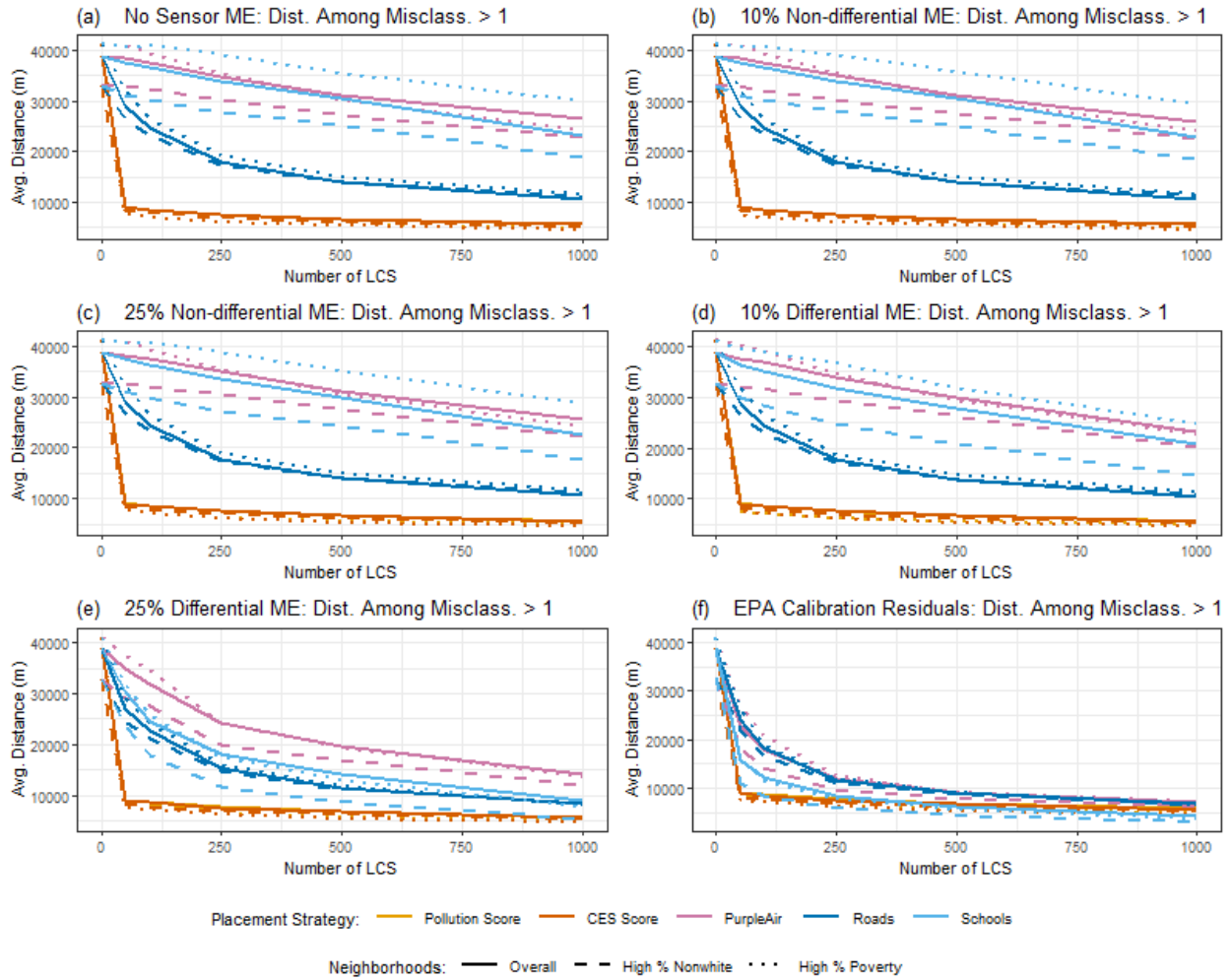
Supplemental Results:

(Originally, this section was in the main text, section 4.3, but was eventually pulled to help streamline the discussion.)

SI Figure 0, which depicts the average distance to the nearest AQ instrument *among grid-days misclassified by more than one AQI level for each simulation scenario*, allows us to dig more deeply (beyond Figures 3 and 4 in the main text) into the sources of AQ reporting errors for observations with the largest errors. Here, high distance values suggest that large misclassifications are more due to distance to the nearest AQ instrument, while low values indicate that large misclassifications are due to either local variability in AQ or sensor measurement error.

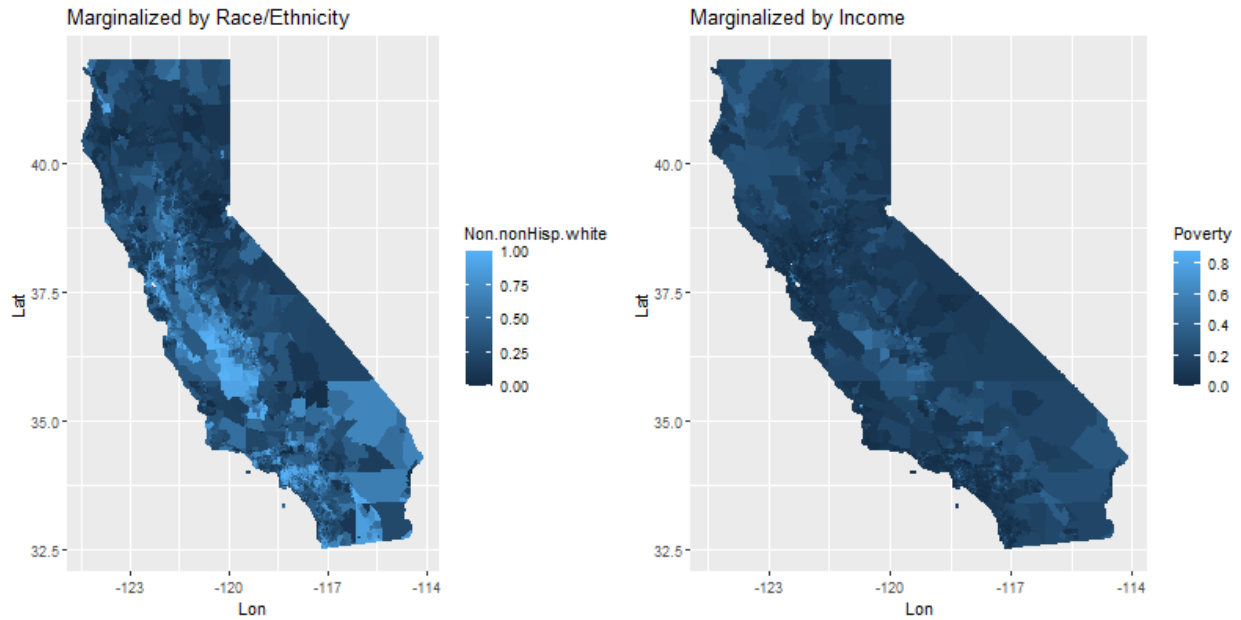
When there is no sensor measurement error (panel a), the distance drops sharply as LCS are added for the CES and Pollution Score-based placements but decreases more gradually for the placements near roads, at schools, and at PurpleAir locations. This indicates that local variability in AQ accounts for a major fraction of large misclassifications under the CES and Pollution Score-based placements. Meanwhile, large misclassifications resulting from near-road placements appear to be due to a combination of local variability and distance to the nearest AQ instrument, and placements at schools and PurpleAir locations are most affected by distance to the nearest AQ instrument (at least, in generating large misclassifications). Another noticeable feature is that for placements at schools and at PurpleAir locations, large misclassifications in CBGs with Q5 % nonwhite tend to be more attributable to local variability than large misclassifications for the population overall, and CBGs with Q5 % poverty tend to experience more large misclassifications due to distance to the nearest AQ instrument than the population overall.

As we add more sensor measurement error, the likelihood of large AQI misclassifications is increased even for individuals living nearer to a sensor. This is illustrated in panels c through f (as sensor measurement error increases) by the steady reductions in distance to nearest monitor among observations with large misclassifications for LCS placements at schools, at PurpleAir locations, and near major roads. LCS placements at schools appear to be more affected by differential measurement error than those at PurpleAir locations or near major roads. This makes sense because school locations in California have higher average PM_{2.5} levels than locations selected by the other two placement strategies (as shown in SI Table B.1).

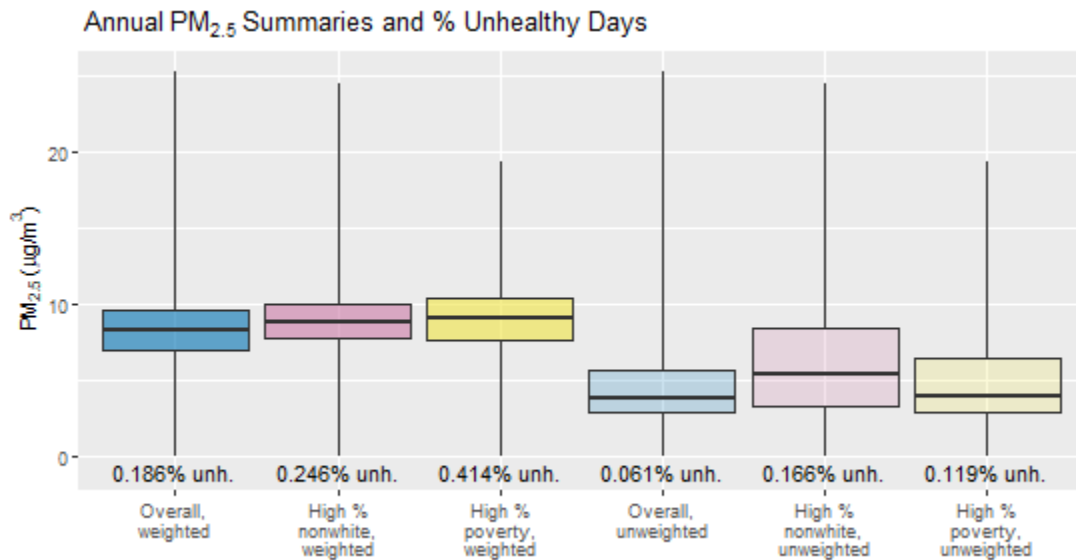


SI Figure 0: Distance to the nearest AQ instrument, among observations misclassified by more than one level of the AQI (e.g. Red to Yellow, or Green to Orange). All results were calculated using 366 days and averaged across 50 simulation trials, weighted by population density.

Appendix A: Supplemental figures and tables for both analyses (weighted and unweighted by population density)



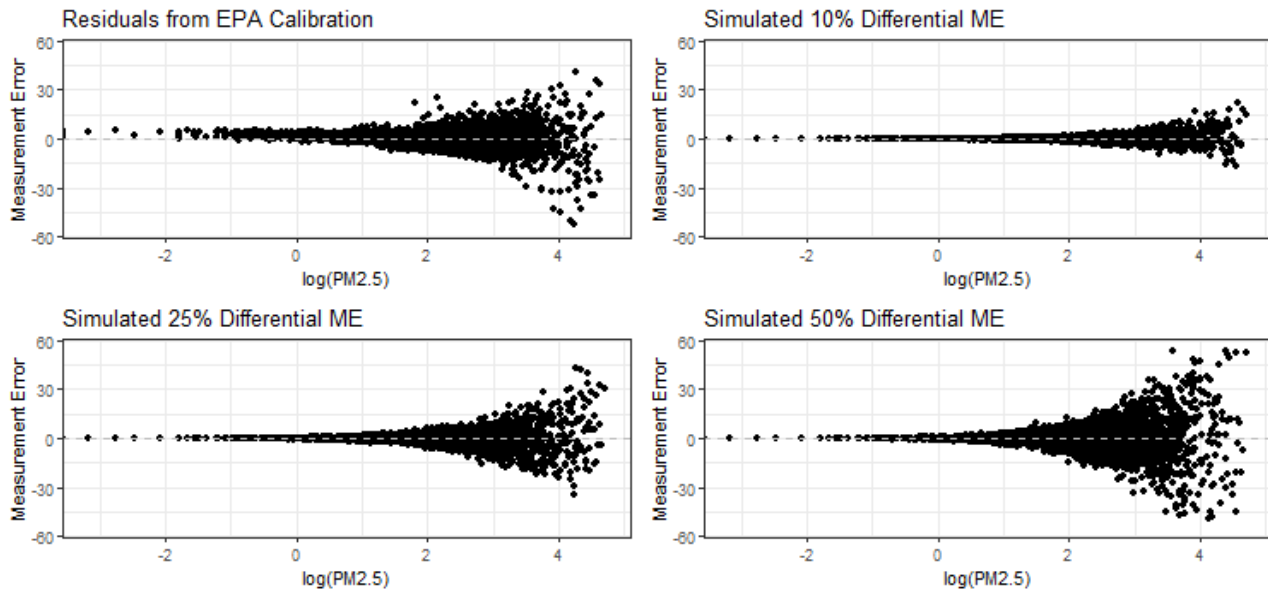
SI Figure A.1: Distribution of marginalized groups used in the analyses: percent of individuals identifying as non-white or Hispanic, and percent of households with income below the poverty line.



SI Figure A.2: Annual average $PM_{2.5}$ ($\mu g/m^3$) summaries for population subsets, weighted and unweighted by population density; labeled with % Unhealthy (AQI classification = Orange and higher) days.

SI Table A.1: Average number of LCS (out of 1,000 deployments) placed in the counties of Sacramento, Imperial, and Los Angeles according to each placement strategy considered in this study.

County	Population size (2016)	Avg. CES Score	Purple Air (current)	Schools	Near road locations	CES Score based	Pollution Score based
Sacramento	1,495,611	23	26	41	10	7	7
Imperial	186,019	38	1	7	27	47	34
Los Angeles	10,180,169	23	106	204	29	25	26



SI Figure A.3: Top left plot shows the empirical distribution of residuals in $\mu\text{g}/\text{m}^3$ (compared to AQS monitor measurements within 50m) from PurpleAir observations corrected using the EPA equation. The other three plots show the distributions resulting from our method of simulating sensor measurement error differentially with respect to true $\text{PM}_{2.5}$ concentration. Note that 50% accuracy was not included in the full analysis simulations.

SI Table A.2: Summary statistics of the Di et al. estimates in each decile of AQS $\text{PM}_{2.5}$ from our correction dataset, in $\mu\text{g}/\text{m}^3$. Matching on these deciles was used to draw empirical residuals from the EPA correction applied to collocated PurpleAir and AQS data.

Decile	Minimum	Q1	Median	Mean	Q3	Maximum
1	0.000	0.684	1.265	1.262	1.863	2.455
2	2.455	2.757	3.074	3.083	3.404	3.750

3	3.750	4.055	4.375	4.389	4.716	5.083
4	5.083	5.385	5.711	5.731	6.066	6.458
5	6.458	6.780	7.136	7.167	7.538	8.000
6	8.000	8.365	8.778	8.818	9.251	9.796
7	9.796	10.225	10.705	10.747	11.246	11.875
8	11.88	12.45	13.15	13.25	13.99	15.08
9	15.08	15.93	17.10	17.60	18.91	22.65
10	22.65	24.24	26.57	29.49	31.02	112.18

Appendix B: Supplemental metrics for analysis weighted by population density

SI Table B.1: Basic descriptive statistics, weighted by population density (unless otherwise specified) and normalized, to provide a sense of scale. Non-normalized results are in SI Table B.1. All cells are of the form “Mean (Standard Deviation)”. Note: Q5 = top quintile; wtd. = weighted. The rows that specify when population density greater than 500 / sq. mile is to account for both the weighting to select the LCS locations (i.e. by proximity to roads, Pollution Score, or CES Score) and the weighting by population density in our results. Population density less than 500 / sq. mile is considered rural by the USDA (<https://www.ers.usda.gov/topics/rural-economy-population/rural-classifications/what-is-rural/>).

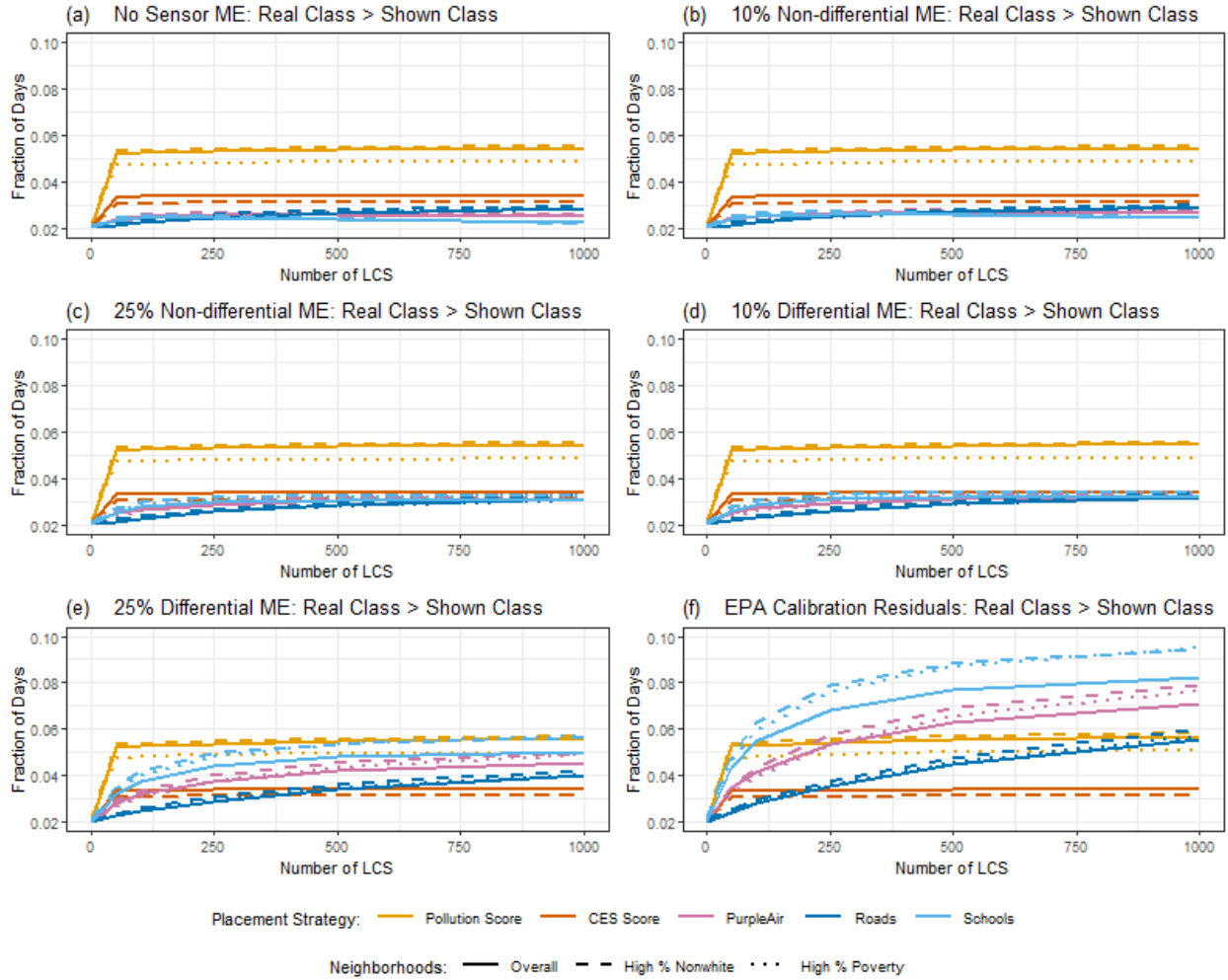
Locations	Annual Avg. PM_{2.5} (μg/m³)	% Poverty	CES Score	% Nonwhite or Hispanic	Population Density (unweighted)
CA overall	0 (1)	0 (1)	0 (1)	0 (1)	0 (1)
EPA monitor sites	0.34 (1.01)	0.67 (1)	0.62 (1.06)	0.22 (0.96)	2.54 (3.99)
PurpleAir sites	-0.24 (0.83)	-0.33 (0.83)	-0.46 (0.9)	-0.26 (0.93)	2.51 (4.11)
School sites	0.23 (0.89)	0.17 (1)	0.23 (1.02)	0.33 (0.93)	3.96 (4.28)
Favoring by nearby roads (not wtd. by pop.)	-1.37 (1.23)	0.08 (0.75)	-0.29 (0.81)	-0.93 (0.96)	0.3 (1.75)

density)					
Favoring by roads, where pop. density > 500	-0.28 (1.06)	-0.08 (1)	-0.16 (0.97)	-0.3 (1)	2.87 (3.67)
Favoring by Pollution Score (not wtd. by pop. density)	-1.7 (1.26)	0.17 (0.67)	-0.1 (0.79)	-0.81 (0.93)	0.02 (1.07)
Favoring by Pollution Score, where pop. density > 500	0 (1.03)	-0.08 (1)	0.03 (1.04)	-0.15 (0.96)	2.81 (3.48)
Favoring by CES Score (not wtd. by pop. density)	-1.67 (1.31)	0.25 (0.75)	0.11 (0.8)	-0.67 (0.96)	0.03 (1.16)
Favoring by CES Score, where pop. density > 500	0.12 (1.06)	0.17 (1.08)	0.41 (1.04)	0.11 (0.93)	3.13 (3.79)
Q5 % nonwhite	0.31 (0.9)	0.33 (1)	0.49 (0.93)	0.78 (0.44)	0.29 (1.83)
Q5 % poverty	0.37 (1.09)	1.5 (0.75)	0.92 (0.9)	0.7 (0.78)	0.02 (1.26)

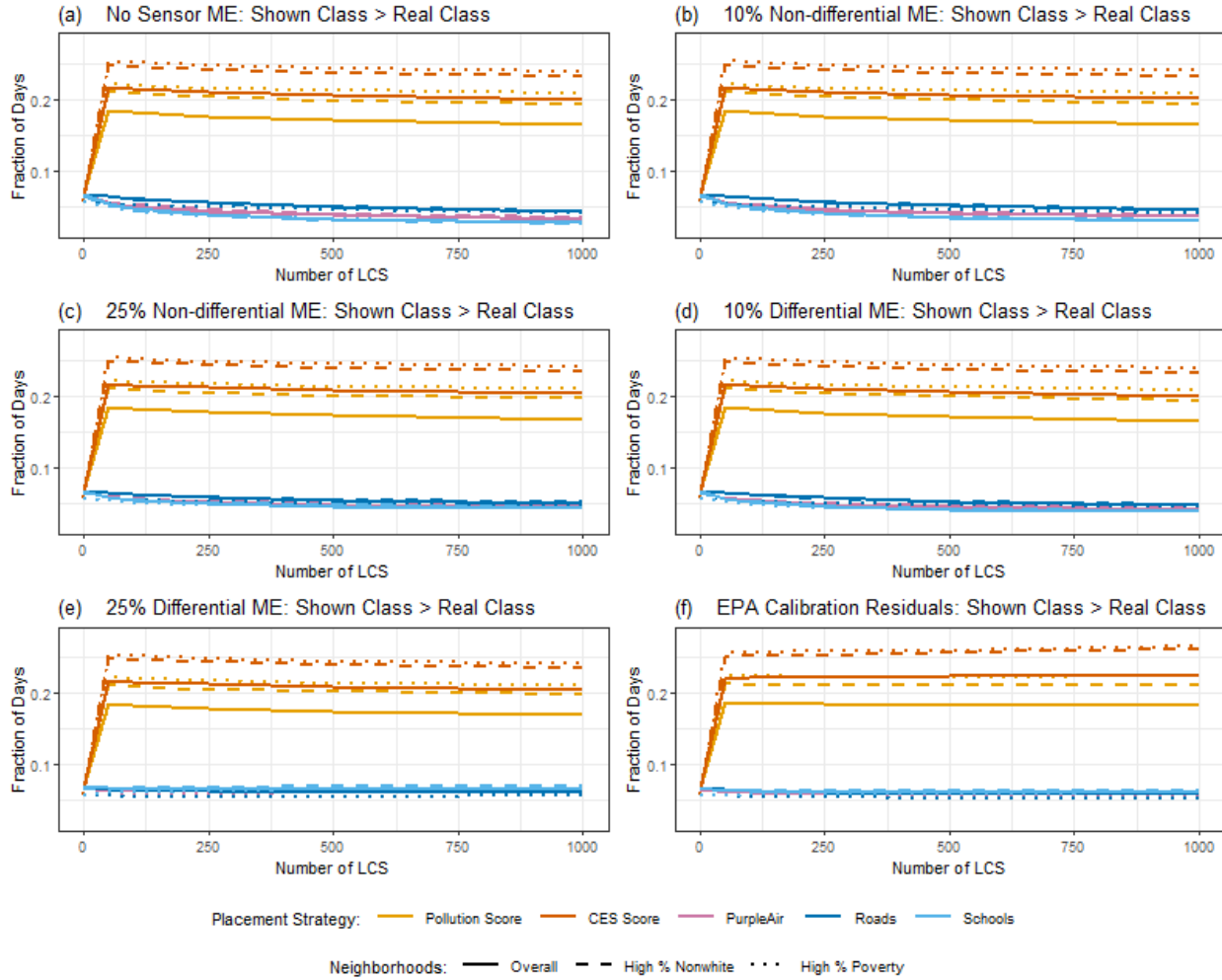
SI Table B.2: Non-normalized version of SI Table B.1 (above). Basic descriptive statistics, weighted by population density (unless otherwise specified). All cells are of the form “Mean (Standard Deviation)”. Note: Q5 = top quintile; wtd. = weighted. The rows that specify when population density greater than 500 / sq. mile is to account for both the weighting to select the LCS locations (i.e. by proximity to roads, Pollution Score, or CES Score) and the weighting by population density in our results. Population density less than 500 / sq. mile is considered rural.

Locations	Annual Avg. PM_{2.5} (μg/m³)	% Poverty	CES Score	% Nonwhite or Hispanic	Population Density (unweighted)
CA overall	8.23 (1.98)	0.16 (0.12)	28.11 (15.93)	0.61 (0.27)	249.81 (1,526.04)
EPA monitor sites	8.91 (2)	0.24 (0.12)	37.98 (16.95)	0.67 (0.26)	4,119.08 (6,090.22)

PurpleAir sites	7.76 (1.65)	0.12 (0.1)	20.84 (14.33)	0.54 (0.25)	4,075.79 (6,267.25)
School sites	8.69 (1.77)	0.18 (0.12)	31.74 (16.28)	0.70 (0.25)	6,296.3 (6,531.5)
Favoring by nearby roads (not wtd. by pop. density)	5.52 (2.43)	0.17 (0.09)	23.42 (12.96)	0.36 (0.26)	701.74 (2,670.86)
Favoring by nearby roads, where pop. density > 500	7.68 (2.1)	0.15 (0.12)	25.63 (15.5)	0.53 (0.27)	4,627.07 (5,604.17)
Favoring by Pollution Score (not wtd. by pop. density)	4.87 (2.49)	0.18 (0.08)	26.52 (12.51)	0.39 (0.25)	275.26 (1,633.18)
Favoring by Pollution Score, where pop. density > 500	8.23 (2.04)	0.15 (0.12)	28.51 (16.57)	0.57 (0.26)	4,535.05 (5,309.65)
Favoring by CES Score (not wtd. by pop. density)	4.93 (2.6)	0.19 (0.09)	29.88 (12.71)	0.43 (0.26)	296.21 (1,774.24)
Favoring by CES Score, where pop. density > 500	8.46 (2.09)	0.18 (0.13)	34.68 (16.54)	0.64 (0.25)	5,027.12 (5,779.83)
Q5 % nonwhite	8.84 (1.78)	0.20 (0.12)	35.92 (14.87)	0.82 (0.12)	696.8 (2,789.15)
Q5 % poverty	8.96 (2.16)	0.34 (0.09)	42.81 (14.28)	0.80 (0.21)	277.93 (1,922)



SI Figure B.1: The average fraction of days on which the real AQI class (what was truly experienced) was higher than the shown AQI class (reported from the nearest monitor or sensor), resulting from different numbers of LCS deployed, LCS placement strategies, and sensor measurement error types and amounts. All results were calculated using 366 days and averaged across 50 simulation trials, weighted by population density.



SI Figure B.2: The average fraction of days on which the shown AQI class (reported from the nearest monitor or sensor) was higher than the real AQI class (what was truly experienced), resulting from different numbers of LCS deployed, LCS placement strategies, and sensor measurement error types and amounts. All results were calculated using 366 days and averaged across 50 simulation trials, weighted by population density.

Appendix C: Results unweighted by population density (main and supplemental metrics)

SI Table C.1: Basic descriptive statistics, counterpart of SI Table B.2, unweighted by population density. All cells are of the form “Mean (Standard Deviation)”. Note: Q5 = top quintile; Wtd. = weighted.

Locations	Annual Avg. PM _{2.5} (μg/m ³)	% Poverty	CES Score	% Nonwhite or Hispanic	Population Density
-----------	--	-----------	-----------	------------------------	--------------------

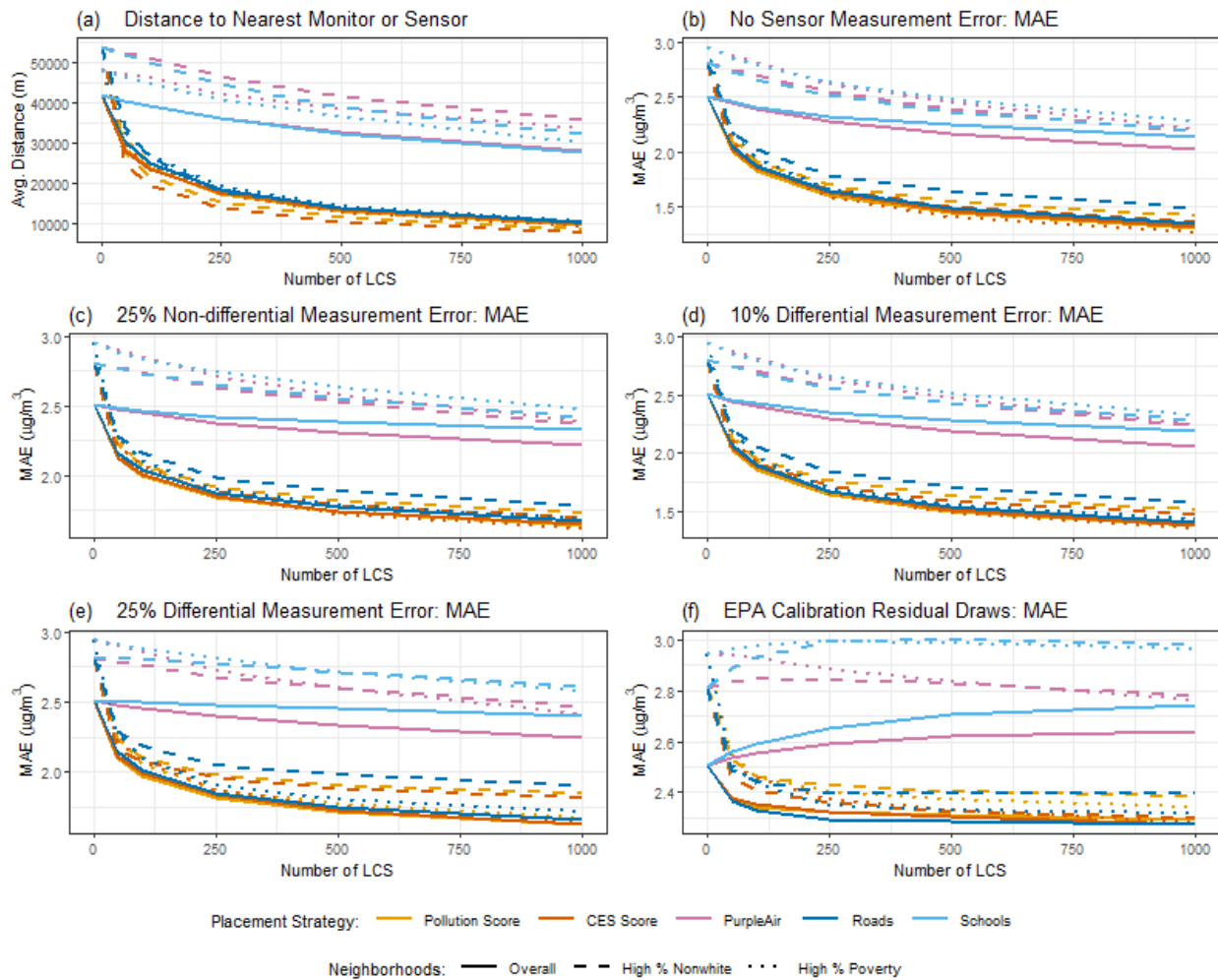
CA overall	4.55 (2.32)	0.17 (0.08)	23.92 (11.95)	0.35 (0.24)	249.81 (1,526.04)
EPA monitor sites	7.43 (2.58)	0.20 (0.13)	29.23 (15.8)	0.53 (0.26)	4,119.08 (6,090.22)
PurpleAir sites	6.63 (2.05)	0.11 (0.09)	16.47 (12.32)	0.38 (0.24)	4,075.79 (6,267.25)
School sites	8.04 (2.08)	0.16 (0.11)	27.88 (16.04)	0.58 (0.27)	6,296.3 (6,531.5)
Favoring by nearby roads	5.52 (2.43)	0.17 (0.09)	23.42 (12.96)	0.36 (0.26)	701.74 (2,670.86)
Favoring by Pollution Score	4.87 (2.49)	0.18 (0.08)	26.52 (12.51)	0.39 (0.25)	275.26 (1,633.18)
Favoring by CES Score	4.93 (2.6)	0.19 (0.09)	29.88 (12.71)	0.43 (0.26)	296.21 (1,774.24)
Q5 % nonwhite	5.77 (2.93)	0.24 (0.09)	38.31 (10.84)	0.74 (0.12)	696.8 (2,789.15)
Q5 % poverty	4.85 (2.66)	0.30 (0.06)	31.6 (13.5)	0.52 (0.26)	277.93 (1,922)

SI Table C.2: Results (unweighted by population density, counterpart of Table 1 in main text) when there are no LCS vs. LCS at all real PurpleAir locations (n = 4,343), assuming different kinds and amounts of sensor measurement error. Results are the average of 50 simulations to account for randomness in the sensor measurement error generation. Unless otherwise specified, “errors” refer to the difference between the true exposure experienced at each grid centroid and the exposure reported from the nearest AQ instrument. AQI under-classification is when the true exposure class is greater than what someone is shown, and over-classification is when the true exposure class is less than what someone is shown. Rate of UH misclassification (UHM) is the fraction of days with unhealthy AQI (Orange+) that are reported as healthy AQI (Green or Yellow).

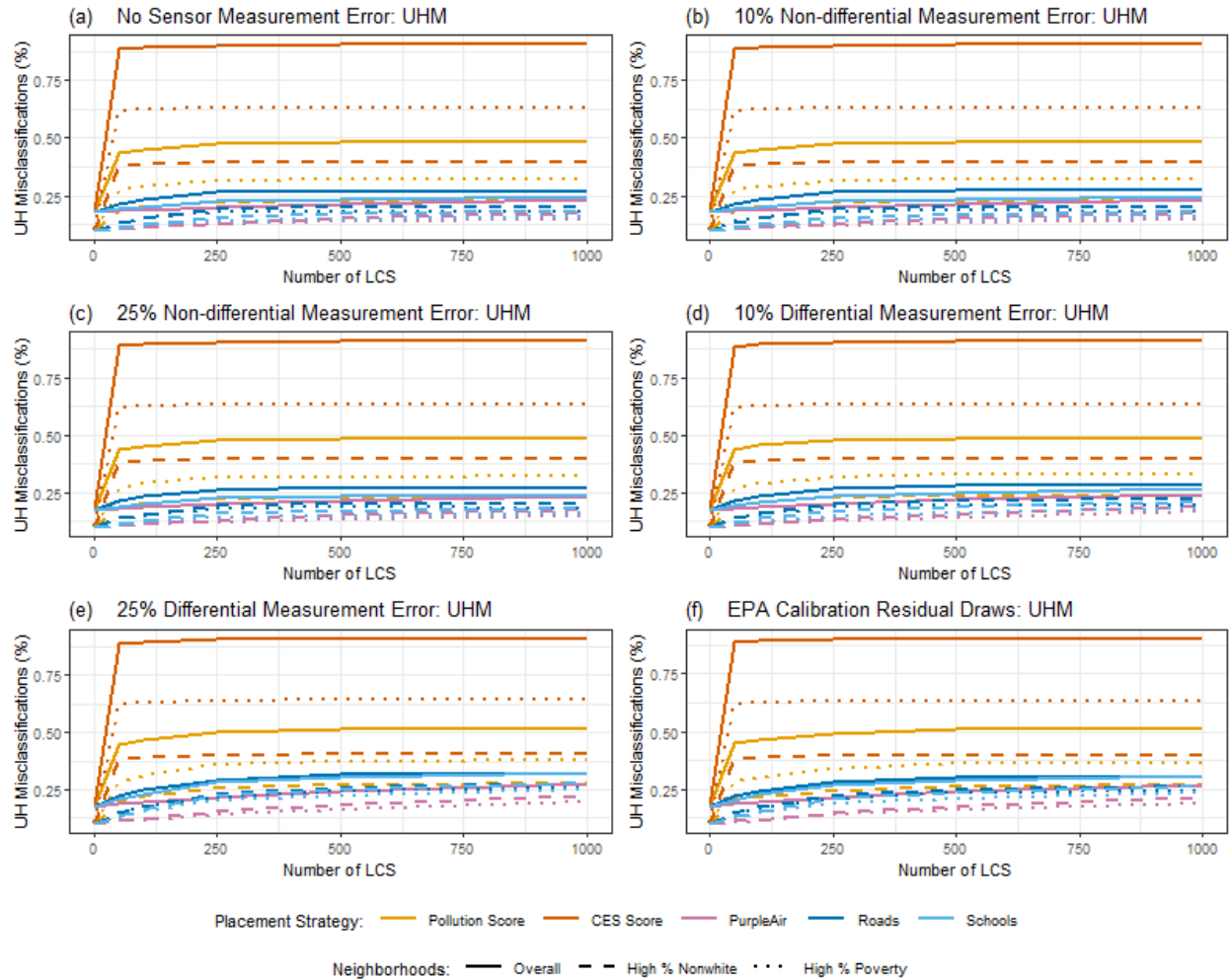
Population	Std. Dev. of Sensor Measurement Error ($\mu\text{g}/\text{m}^3$)	MAE ($\mu\text{g}/\text{m}^3$)	95th Percentile of Errors ($\mu\text{g}/\text{m}^3$)	Under-classified AQI (%)	Over-classified AQI (%)	UHM (%)
No LCS						
Overall	—	2.51	8.08	1.17	7.09	17.67

Q5 % nonwhite	—	2.81	9.43	1.58	10.56	9.86
Q5 % poverty	—	2.95	9.40	1.11	9.63	9.89
No Sensor Measurement Error						
Overall	0	1.79	5.87	1.36	3.59	25.95
Q5 % nonwhite	0	1.79	5.60	2.11	3.76	21.41
Q5 % poverty	0	1.83	5.88	1.58	3.11	16.82
10% Non-differential Measurement Error						
Overall	0.5	1.85	5.92	1.39	3.66	25.57
Q5 % nonwhite	0.5	1.84	5.65	2.19	3.86	20.76
Q5 % poverty	0.5	1.89	5.94	1.63	3.17	15.80
25% Non-differential Measurement Error						
Overall	1.25	2.08	6.20	1.47	4.09	25.58
Q5 % nonwhite	1.25	2.07	5.95	2.36	4.42	21.13
Q5 % poverty	1.25	2.11	6.21	1.73	3.64	16.25
10% Differential Measurement Error						
Overall	0.78	1.86	5.99	1.51	3.84	27.04
Q5 % nonwhite	0.91	1.88	5.75	2.44	4.14	23.14
Q5 % poverty	0.88	1.90	6.00	1.79	3.38	18.38
25% Differential Measurement Error						
Overall	1.95	2.12	6.69	1.85	4.85	32.78
Q5 % nonwhite	2.27	2.23	6.66	3.12	5.50	29.41

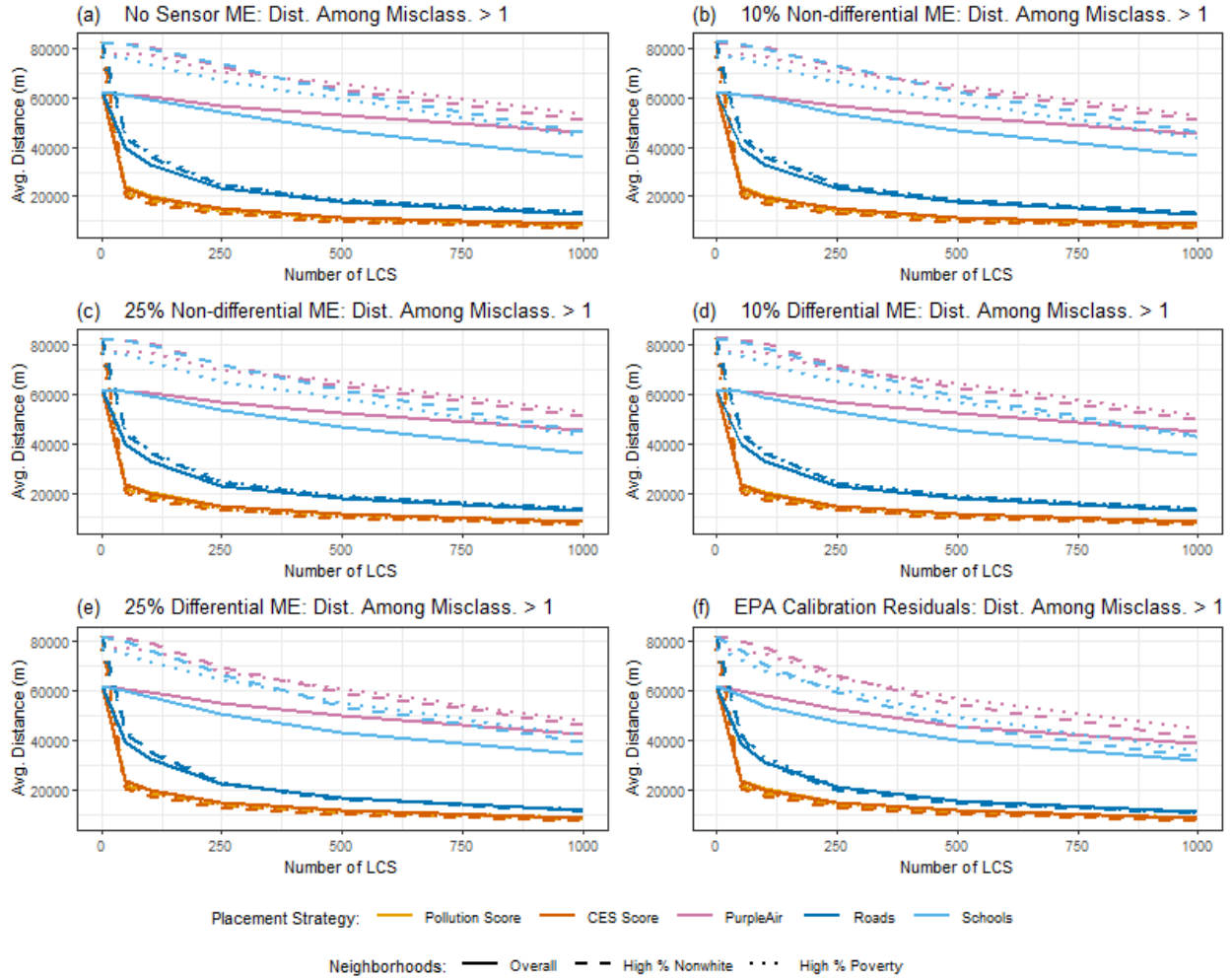
Q5 % poverty	2.20	2.18	6.71	2.20	4.56	24.72
EPA Correction Residual Decile Draws						
Overall	3.06	2.68	7.33	2.62	4.61	30.93
Q5 % nonwhite	3.43	2.72	7.56	4.50	5.24	27.50
Q5 % poverty	3.38	2.69	7.37	3.11	4.41	23.34



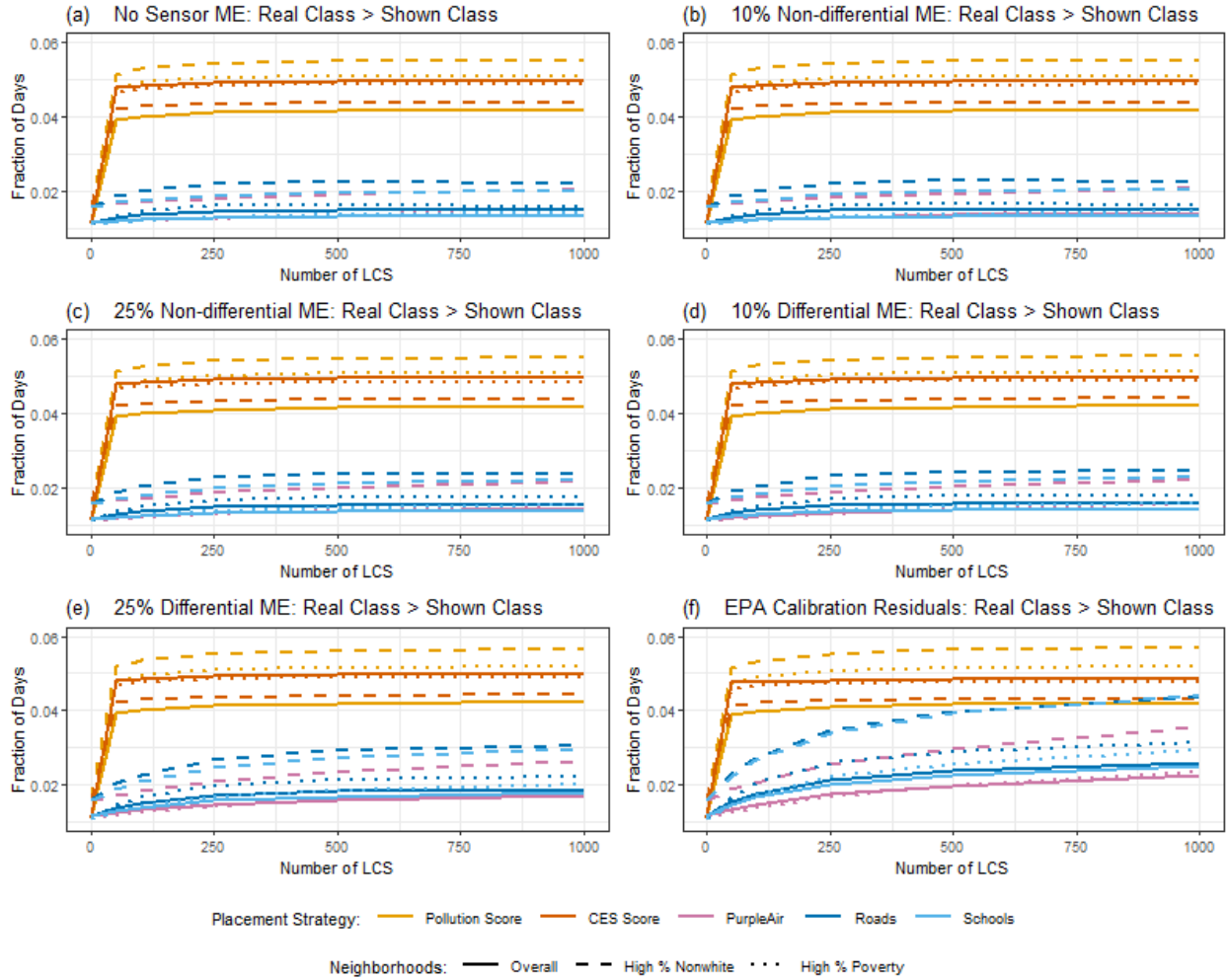
SI Figure C.1: Distance to the nearest monitor or sensor and mean absolute error (between what is reported vs. experienced) resulting from different numbers of LCS deployed, LCS placement strategies, and sensor measurement error types and amounts. All results were calculated using 366 days and averaged across 50 simulation trials, unweighted by population density.



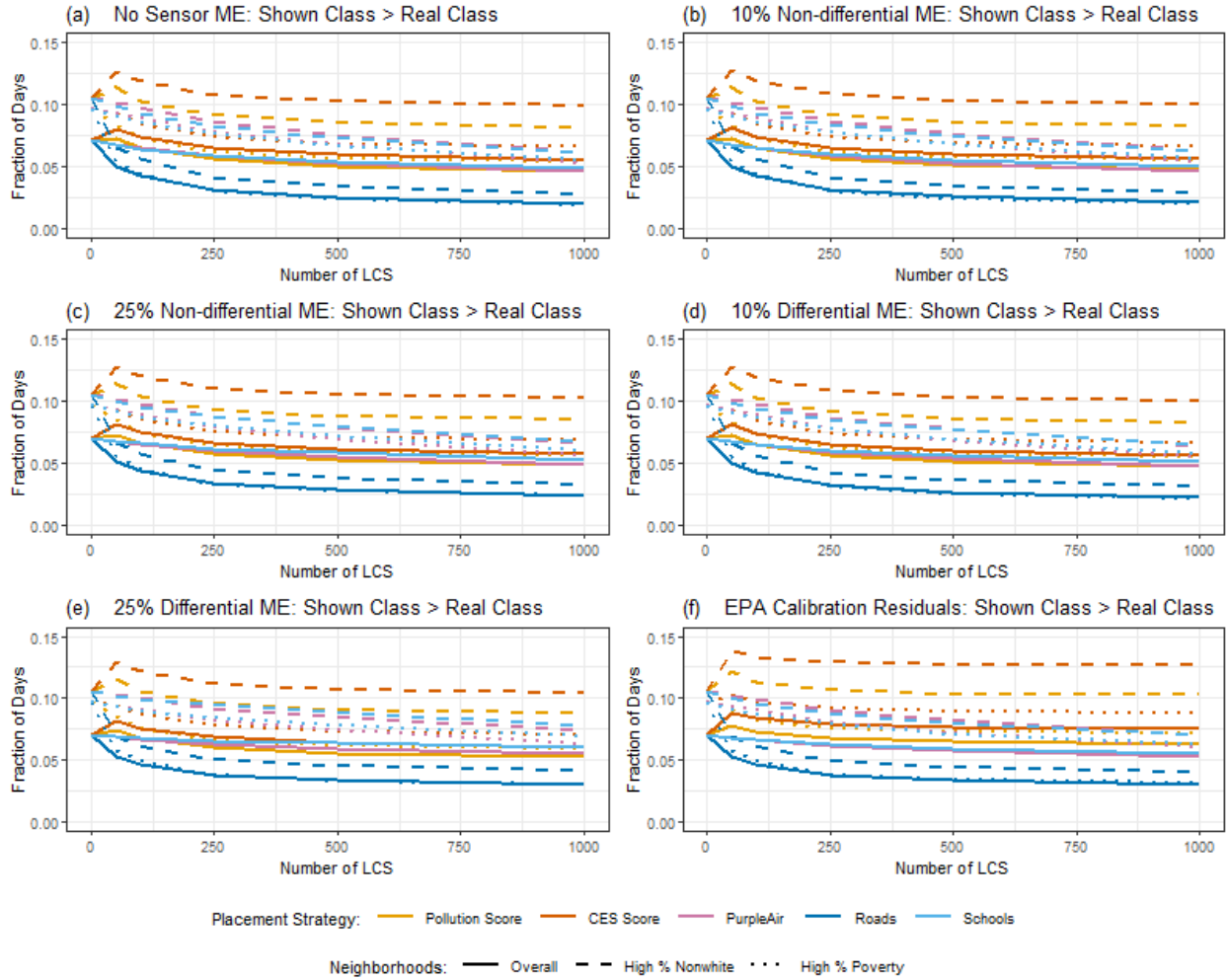
SI Figure C.2: Rates of UH misclassification resulting from different numbers of LCS deployed, LCS placement strategies, and sensor measurement error types and amounts. UH misclassification occurs when the air quality is unhealthy (Orange+) but is reported as healthy (Green or Yellow); the UHM rate is calculated by dividing the fraction of UH misclassifications by the total fraction of unhealthy days experienced by each group. All results were calculated using 366 days and averaged across 50 simulation trials, unweighted by population density.



SI Figure C.3: Distance to the nearest monitor or sensor, among observations misclassified by more than one level of the AQI (e.g. Red to Yellow, or Green to Orange). All results were calculated using 366 days and averaged across 50 simulation trials, unweighted by population density.



SI Figure C.4: The average fraction of days on which the real AQI class (what was truly experienced) was higher than the shown AQI class (reported from the nearest monitor or sensor), resulting from different numbers of LCS deployed, LCS placement strategies, and sensor measurement error types and amounts. All results were calculated using 366 days and averaged across 50 simulation trials, unweighted by population density.



SI Figure C.5: The average fraction of days on which the shown AQI class (reported from the nearest monitor or sensor) was higher than the real AQI class (what was truly experienced), resulting from different numbers of LCS deployed, LCS placement strategies, and sensor measurement error types and amounts. All results were calculated using 366 days and averaged across 50 simulation trials, unweighted by population density.